THE ROLE OF MENIN IN THE PATHOPHYSIOLOGY OF CHOLESTATIC LIVER DISEASE AND CHOLANGIOCARCINOMA

A Dissertation

by

LAURENT JIRI HOLL EHRLICH

Submitted to the Office of Graduate and Professional
Studies of Texas A&M University
In partial fulfillment of the requirements for the degree of

DOCTOR OF PHILOSOPHY

Chair of Committee,	Shannon Glaser
Committee Members,	Gianfranco Alpini
	Fanyin Meng
	Cynthia Meininger
	David Dostal
Head of Department,	Warren Zimmer

May 2019

Major Subject: Medical Sciences

ABSTRACT

Multiple Endocrine Neoplasia type I (MEN1) is a familial cancer syndrome of the parathyroid glands, pituitary glands, and pancreatic islet cells. Recent evidence has pointed towards a more comprehensive role for menin, the tumor suppressor encoded by the MEN1 gene, in human disease. Cholangiocytes, the epithelial cells lining the bile ducts, become reactive and adopt a neuroendocrine-like phenotype following injury. Since menin has been identified as a tumor suppressor in neuroendocrine-type cancers, we hypothesized that menin may play a role in cholestatic liver disease. Thus, we explored the effects of menin on proliferation, angiogenesis, and fibrosis in several models of cholestatic liver disease as well as cholangiocarcinoma (CCA). Our studies used bile-duct ligation (BDL) and MDR2$^{-/-}$ cholestatic mouse models to study the effects of menin on extrahepatic obstruction and primary sclerosing cholangitis (PSC), respectively. Menin was upregulated using a miR-24 vivo-morpholino, and a menin-MLL inhibitor (MI-2-2) was used to block MLL-dependent menin function. Menin was overexpressed *in vitro* in human CCA cell lines, cells were implanted into nude mice, and animals assessed for tumor burden. Immunohistochemistry (IHC) was performed to measure intrahepatic bile duct mass (IBDM) via CK-19 staining, and Sirius Red staining was performed to measure collagen deposition and fibrosis. Menin expression was measured by real-time PCR and flow cytometry. The fibrotic expression markers fibronectin 1 (FN1), collagen type 1 alpha1 (Col1α1), transforming growth factor-β1 (TGF-β1), and α-smooth muscle actin (α-SMA), as well as proliferative (Ki67) and angiogenic

expression markers (VEGFA/C, VEGFR2/3, ANG1/2, TIE1/2) were measured by real-time polymerase chain reaction (PCR). Finally, we assessed alpha7 nicotinic acetylcholine receptor (α7-nAChR) axis activation upstream of menin function using an α7-nAChR$^{-/-}$ BDL mouse model, and an *in vitro* mechanical stretch system that mimics increased biliary pressure. We found that menin function was positively associated with hepatic fibrosis in cholestatic liver disease and CCA. However, menin overexpression decreased tumor burden in xenograft tumor models. The α7-nAChR expression increases following BDL, and α7-nAChR$^{-/-}$ mice are protected from BDL induced hepatic damage, fibrosis, and biliary proliferation. Mechanical stress increases menin expression, which is abrogated in α7-nAChR$^{-/-}$ cells. We conclude that the role of menin in cholangiocyte disease can be dichotomous. Loss of menin is detrimental in CCA, but potentially ameliorative in fibrotic-type cholestatic disease. The use of small-molecule inhibitors such as MI-2-2, miR-24 and/or histone deacetylase inhibitors can shed light on menin's mechanism of action and function and could potentially be used as novel targeted therapies.

ACKNOWLEDGMENTS

I acknowledge my mentor Dr. Shannon Glaser for providing continued support and guidance throughout my time in the lab. I have learned a great deal about the rigor of the scientific process as a result. Additionally, I thank Dr. Gianfranco Alpini for providing invaluable input and feedback to support my dissertation research.

I acknowledge the investigators of Baylor Scott and White Digestive Diseases Research Center, the Central Texas Veterans Health Care System, and Texas A&M College of Medicine, particularly Drs. Fanyin Meng, David Dostal, and Vincent Van Buren who have helped me with a variety of crucial skill sets including both experimental and bioinformatics approaches. I also thank Dr. Cynthia Meininger for unwavering support throughout the hectic Ph.D. process. Additionally, I thank Dr. Terry C. Lairmore for introducing me to the lab as well as providing clinical context to the research and Dr. Sharon DeMorrow for assisting in the committee process.

I acknowledge current and former members of the Digestive Diseases Research Center and the Department of Medical Physiology who helped with these studies. These include Julie Venter, April O'Brien, Tori Sheppard, Tianhao Zhou, Konstantina Kyritsi, Dr. Damir Nizamutdinov, and Dr. Chad Hall. I also thank my family members for always supporting me, and my sister and brother, Elena Ehrlich and Andre Ehrlich, respectively, for helping me with bioinformatics analysis.

Last but not least, I acknowledge the Texas A&M Health Science Center College M.D./Ph.D. program for providing me this opportunity of pursuing a career as a physician-scientist. I also acknowledge the National Institute of Health, Baylor Scott and White Health, and Central Texas Veterans Health Care System for providing the resources to perform these studies.

CONTRIBUTORS AND FUNDING SOURCES

Contributors

Part 1, faculty committee recognition

This work was supervised by a dissertation committee consisting of Professor Shannon Glaser [committee chair], Distinguished Professor Gianfranco Alpini, Professor Cynthia Meininger, and Professor David Dostal and Associate Professor Fanyin Meng of the Department of Medical Physiology as well as Professor Dr. Terry C. Lairmore.

Part 2, student/collaborator contributions

All work reported in this dissertation was completed by the student under the supervision of Dr. Shannon Glaser and Dr. Gianfranco Alpini of the Department of Medical Physiology.

Funding Sources

Graduate study was supported by the Texas A&M Health Science Center College of Medicine M.D./Ph.D. program, the Dr. Nicholas C. Hightower Centennial Chair of Gastroenterology from Scott & White, a Veterans Administration Research Career Scientist Award, a Veterans Administration Merit award to Dr. Alpini (5I01BX000574), a Veterans Administration Merit Award (5I01BX002192) to Dr. Glaser, and the National Institutes of Health grants DK58411, DK07698, and DK062975 to Drs. Alpini and Glaser. This research is the result of work supported by resources at the Central

Texas Veterans Health Care System. The content is the responsibility of the author(s) alone and does not necessarily reflect the views or policies of the Department of Veterans Affairs of the United States Government.

TABLE OF CONTENTS

LIST OF FIGURES

1. INTRODUCTION [1]

Cholangiocytes are specialized epithelial cells that line hepatic bile ducts and function to modify the passage of bile with water and electrolytes and nullify xenobiotics and microbiota (1,2). Bile is initially secreted by hepatocytes into specialized interstitial spaces called bile canaliculi that are sealed by tight junctions. Bile flows towards the portal tracts where it first enters the small intrahepatic biliary tree lined with small cholangiocytes (8 μm) at the Canals of Herring. The biliary tree becomes progressively larger to form large intrahepatic bile ducts, lined by large cholangiocytes (15 μm), and ultimately extrahepatic bile ducts empty bile into the duodenum (3,4). Large and small cholangiocytes, lining large and small bile ducts, respectively, exhibit distinct morphological, functional, and proliferative features that vary based on the disease state (3-5).

Diseases targeting cholangiocytes, termed cholangiopathies, lead to cholestasis, increased biliary pressure, hepatic fibrosis, and chronic inflammation that can trigger cirrhosis or malignant transformation (6). Cholestasis refers to the accumulation of bile in hepatic tissue following intrahepatic or extrahepatic biliary obstruction. Extrahepatic obstruction can be caused by gallstones, pancreatic ductal adenocarcinoma, strictures, or cholangiocarcinoma, whereas intrahepatic biliary diseases include primary biliary cholangitis (PBC), primary sclerosing cholangitis (PSC), and polycystic liver

[1] § Part of this chapter is reprinted with permission from L. Ehrlich, C. Hall, F. Meng, T. Lairmore, G. Alpini, and S. Glaser, A Review of the Scaffold Protein Menin and its Role in Hepatobiliary Pathology, Gene Expression, vol. 17, no. 3, pp 251263, 2017. ©2017 Cognizant, Inc

disease (7). Cholangiopathies are commonly characterized by four main stages of disease. Disease progression begins with portal hepatitis and inflammation with bile duct destruction. This is followed by periportal hepatitis and bile duct proliferation, which can progress to fibrous septa or bridging necrosis in the liver and eventually stage four, cirrhosis (8). During late stages of disease, the balance between proliferation and cholangiocyte death is disturbed, leading to ductopenia and further hepatic fibrosis (1). However chronic inflammation can also cause cholangiocyte hyperplasia resulting in an increased risk for malignant transformation, especially in PSC (6). Symptoms of cholangiopathies are reflective of the cholestatic process and eventual loss of liver function including fatigue, pruritus, portal hypertension and xanthomas, can occur (8). Current treatment options are limited to ursodeoxycholic acid (UCDA) supplementation, providing the best improvement in PBC patients (1).

Cirrhosis is an end-stage, irreversible liver scarring and the leading cause of liver failure for which the current mainstay of treatment is liver transplantation. There is currently an 80% mortality rate without transplantation once full hepatic failure ensues (7, 9). Major consequences of cirrhosis include portal hypertension and its effects such as ascites, variceal bleeding, hepatic encephalopathy, renal failure, and, of course, cancer (10). Liver fibrosis or scar formation is characterized by abnormal accumulation of extracellular matrix and further progression to cirrhosis involves diffuse scarring with dense fibrous septations around regenerating hepatocytes (7). The onset of liver fibrosis begins with injury or insult to either the hepatic parenchyma or the biliary epithelium, as seen in cholestatic disease. In the face of chronic injury, hepatocyte regeneration is

no longer sufficient and ductular proliferation of intrahepatic bile ducts takes place. An increased population of cholangiocytes accumulates at the border of the bile ducts and hepatic parenchyma, contributing to the progression of liver fibrosis through the recruitment of fibrogenic cells (1,7). The etiology of injury plays a role in the cirrhotic pattern, with biliary fibrosis inducing toxic bile acid accumulation that leads to inflammation and activation of cholangiocytes and myofibroblasts that cause a portal-portal fibrotic picture (10).

The anatomical features and the microenvironment surrounding cholangiocytes play an important role in its pathophysiology. The apical sides of cholangiocytes facing the ductal lumen possess single, primary cilia that both sense the composition of passing bile and physically help push it along (5). Additionally, cholangiocyte epithelia are linked by tight junctions to prevent backflow of water, solutes, and/or toxins. The epithelial barrier can become leaky over the course of injury and lead to the regurgitation of toxic substances back into the hepatic parenchyma. Biliary epithelium sits atop a basement membrane that separates it from a matrix of proteoglycans and fibrous proteins produced and maintained by portal mesenchymal and fibroblast cells (11). Proteoglycan fibers hold a large amount of water taking on a gel-like consistency that gives tissue the ability to withstand compressive forces. In contrast, fibrous proteins are more rigid and provide resistance to stretching forces. The major family of fibrous proteins found in the extracellular matrix (ECM) is collagen (which causes fibrosis when overproduced in disease states), however other fibrous proteins are important as well, including fibronectin, elastin, and laminin (11). The ECM also stores latent

signaling ligands for the TGF-β1 pathway that become activated following injury or changes in the microenvironment.

Following cholestatic liver injury, cholangiocytes become reactive and adopt a neuroendocrine-like phenotype by secreting and responding to a number of peptides in both autocrine and paracrine fashion (see Table 1 for a comprehensive list of signaling pathways). Almost all models of biliary injury trigger cholangiocyte proliferation, a process deemed ductular reaction. Multiple cell types involved in this process, and the type of liver injury determines how ductular reaction takes shape. For example, following bile-duct ligation (BDL), a mouse model for extrahepatic cholestasis, large cholangiocytes respond by undergoing mitosis and proliferating while small cholangiocytes transdifferentiate into large cholangiocytes. Distinct signaling mechanisms regulate these disparate outcomes. In this model, large cholangiocytes respond to increased secretin-secretin receptor cognate interactions to boost intracellular cAMP levels and trigger the PKA/Src/MEK/ERK1/1 pathway (12). This has pleiotropic effects ranging from secretion of a bicarbonate umbrella (13) to derepression of VEGF and NGF through downregulation of miR-125b and let7a to promote proliferation (14). In contrast, small cholangiocytes are characterized by activation of the IP3/Ca^{2+}/calmodulin A key step in the initiation of liver fibrosis is activation of cells that transform into myofibroblasts (9). In certain models of biliary injury, activated cholangiocytes can recruit inflammatory cells and myofibroblasts to the site of injury where they secrete ECM components and pro-inflammatory, pro-fibrotic cytokines that causes scarring and fibrosis (7, 9). Several sources of myofibroblasts have been

identified, including hepatic stellate cells (HSCs) and portal fibroblasts. While epithelial cells (i.e. cholangiocytes) do not undergo epithelial to mesenchymal transition (EMT), they can assume a pro-fibrogenic, non-cuboidal phenotype (16).

Table 1: A list of extracellular hepatic neurohormones, neuropeptides, and autonomic innervation signaling with corresponding changes in intracellular signaling and functional outcome

Extracellular Signal	**Intracellular Signal**	**Functional Outcome**
Secretin	↑ cAMP	↑ large cholangiocyte proliferation / fibrosis / ductular secretion
	↑ Ca^{2+}	↑ small cholangiocyte proliferation
Gastrin	↓ cAMP	↓ ductular secretion
TGR5/FXR	↑ cAMP	↑ ductular secretion
α1	↑ PLC/ Ca^{2+}	↑ proliferation / activation of HSCs and small cholangiocytes
α2	↓ cAMP	
β 1-3	↑ cAMP	↑ inflammation / fibrosis
AT1	↑ PKA/ERK1/2/pCREB	↑ cholangiocyte proliferation
AVP	↑ cAMP	↑ cholangiocyte proliferation
M3	↑ cAMP	↑ cholangiocyte proliferation
	↑LJ3K/MEK	↑ HSC proliferation
α7nAChR	↑ Ca^{2+}/ERK1/2	↑ cholangiocyte proliferation
Melatonin-MT1	↓ cAMP/PKA	↓ proliferation / ductular secretion
α-CGRP	↑ cAMP/PKA/CREB	↓ inflammation
SP	↑ cAMP/PKA/CREB	↑ cholangiocyte proliferation / fibrosis, apoptosis
NPY	-	↑ HSC / myofibroblast proliferation / activation
	IP3/ Ca^{2+}/PKC	↓ cholangiocyte proliferation
H1	IP3/CAMK1/CREB	↑ small cholangiocyte proliferation
H2	↑ cAMP	↑ large cholangiocyte proliferation

TGR5, Takeda G-protein-coupled receptor 5; α-adrenergic; β-adrenergic; AT1, Angiotensin I; AVP, arginine vasopressin; M3, muscarinic III; α-CGRP, alpha calcitonin gene-related peptide; SP, substance P; NPY, neuropeptide Y; H, histamine receptor

.

The protein menin was originally studied within the context of multiple endocrine neoplasia type 1 (MEN1), a rare hereditary autosomal dominant tumor syndrome (17). MEN1 syndrome penetrance and expressivity is variable, even among patients from the same family tree. The most common manifestation (100% penetrance by age 50) is primary hyperparathyroidism followed by the development of anterior pituitary adenomas (10- 60% penetrance) (18). Pancreatic neuroendocrine tumors, thymic or bronchial carcinoid tumors, and adrenocortical tumors account for a significant remainder of the morbidity and mortality seen in MEN1 syndrome (19). Additionally, nonendocrine tumors such as angiofibromas, collagenomas, lipomas, and melanomas are common manifestations (18). Emerging evidence points to more clinically subtle complications of MEN1 syndrome, possibly due to hormonal imbalances as a result of neuroendocrine growths. Patients often suffer from kidney and bone disease, premature cardiovascular disease, insulin resistance, and glucose intolerance (20).

Menin is a 67 kilodalton nuclear protein coded by 10 exons spanning 9 kb of genomic sequence and expressed ubiquitously. Patients with MEN1 syndrome inherit a mutated MEN1 allele (11q13) from one of their parents. A tissue-specific somatic mutation in the remaining functional allele, or second hit, results in complete loss of menin expression and organ tumorigenesis. Diagnosis of MEN1 syndrome is validated by identification of a mutation in the exon-coding region or intron-exon junctions of the MEN1 gene locus (19). One genomic analysis of >1300 MEN1 patients revealed that over 70% of mutations lead to truncated or non- existent forms of menin (21). Inhibition of the proteasome-ubiquitin pathway can restore protein expression in some cases (22).

It should be noted that not all MEN1 families have a mutation in the MEN1 coding region, indicating a need to understand the regulatory elements surrounding menin expression and function. Thus, it appears that other genetic and environmental factors play a role in the MEN1 syndrome disease process.

Phylogenetically, menin is evolutionarily conserved among vertebrates and Drosophila, however its amino acid sequence does share homology with other known proteins (23). Mounting evidence points to its role as a scaffold protein with many direct and indirect binding partners (23). For example, menin associates with many hundreds of loci on the mammalian genome despite its lack of a known DNA binding sequence (24). It is generally agreed that menin's primary role is to regulate chromatin architecture through histone modifications, resulting in altered gene transcription or even DNA repair (23). Menin has been shown to directly bind and facilitate function of JunD, an AP-1 transcription factor responsible for histone deacetylation and gene silencing. Menin has also been shown to enable transcription of mixed-lineage leukemia (MLL) protein target genes by modifying histones with activating trimethylation marks (25, 26).

While absolute loss of menin expression is required for MEN1 syndrome tumorigenesis, relative menin expression has since been implicated in cellular proliferation of gastric mucosa, liver, breast, and prostate epithelia, lung adenocarcinoma, and myeloid blasts (27-30). However, its function is tissue and pathway specific. For instance, it is oncogenic in certain leukemias and prostate cancers but it acts as a tumor suppressor in canonical MEN1 syndrome organ sites. Furthermore, menin can act through distinct

signaling pathways, such as NF-$\kappa\beta$ and TGF-β1, and affect diverse functional outcomes such as apoptosis, cell cycle, gene transcription, and DNA repair (23, 29, 31). It remains unclear why tumors arise only in neuroendocrine organs and no other tissue types in patients with MEN1 syndrome. Furthermore, the surrounding regulatory elements that allow variable expressivity and penetrance seen in MEN1 syndrome are not yet understood.

Menin has been linked to TGF-β1 and hepatic stellate cell- (HSC-) driven fibrosis (32). Menin expression was associated with HSC activation and positively correlated with pro-fibrotic collagen and metallopeptidase inhibitor gene expression, both TGF-β1/SMAD transcription targets. Furthermore, TGF-β1 increased menin expression in both hepatocytes and HSCs (32 , 33). Menin expression was increased in human hepatocellular carcinoma (HCC) that had developed within the setting of cirrhosis. A separate study showed that menin drives HCC formation through epigenetic upregulation of Yes-associated protein (YAP) which itself has a diverse array of functions, including antagonism of the SMAD-associated TGF-β1 pathway (34). However, this contradicts menin's canonical role as a tumor suppressor (29). One study has shown that menin expression is downregulated in HCC, and *in vitro* overexpression in HCC cell lines decreased cell proliferation and NF-κB-dependent inflammatory cytokine production (29). Further studies may shed light on menin's role in balancing proliferation and fibrosis during HCC development and progression.

There is a similar mechanism already well-documented in MEN1 syndrome-induced

parathyroid hyperplasia. Much like injured cholangiocytes, parathyroid endocrine cells secrete and respond to TGF-β1 in an autocrine and paracrine manner to regulate parathyroid proliferation. Loss of MEN1 expression, the cause of MEN1 syndrome, prevents TGF-β1 anti- proliferative signaling cascade leading to parathyroid hyperplasia and hyperparathyroidism (35). In contrast, however, TGF-β1 is more involved with hepatic fibrosis and EMT then cholangiocyte proliferation. Thus, it follows logically that MEN1 expression facilitates TGF-β- dependent hepatic fibrosis, and that targeting MEN1 pathways may help ameliorate the fibrotic phenotype.

Why MEN1 disease manifestation is restricted to neuroendocrine organs, pituitary, parathyroid, and islets of the pancreas, remains a mystery, and one that is echoed in menin's conflicting roles during hepatic tumorigenesis and fibrosis. Given menin's role as a scaffold protein involved in chromatin remodeling, it is tempting to envision menin as a key player in epigenetic regulation of cell type identity and, more relevantly, differing responses and outcomes to distinct models of cell injury. The following studies were designed to characterize the role of menin in cholestatic and cholangiocarcinoma disease models and to establish effective treatment modalities to target menin expression and/or function.

2. MENIN DRIVES HEPATIC FIBROSIS IN CHOLESTATIC LIVER DISEASE [2]

2.1 Overview

Liver transplantation remains the primary treatment for primary sclerosing cholangitis (PSC), one of several cholangiopathies that result in cholestatic liver disease. Mdr2$^{-/-}$ mice provide an *in vivo* model of PSC with characteristic biliary inflammation and fibrosis that subsequently develop cirrhosis and hepatic malignancies. Since cholangiocytes express a neuroendocrine phenotype within the liver, we tested the hypothesis that the tumor suppressor protein menin is implicated in the progression of liver fibrosis and that menin expression can be regulated in the liver via miR-24. Menin expression was measured in human PSC, Mdr2$^{-/-}$, and bile-duct ligated (BDL) mice. Twelve-week old Mdr2$^{-/-}$ mice were treated with miR-24 Vivo Morpholino (miR-24 VM) to knockdown miR-24 expression levels, and menin function was targeted in BDL mice with a menin-MLL inhibitor. Liver fibrosis was evaluated using Sirius Red staining, hydroxyproline assay, and qPCR for genes associated with liver fibrosis (fibronectin 1 (FN1), collagen type 1 alpha1 (Col1α1), transforming growth factor-β1 (TGF-β1), and α-smooth muscle actin (α-SMA)). Studies were replicated *in vitro* using mouse cholangiocytes and human hepatic stellate cells treated with miR-24 hairpin inhibitor and mimic. Menin and miR-24 gene expression measured via qPCR. Menin

[2] § Part of this chapter is reprinted with permission from C. Hall, L. Ehrlich, F. Meng, P. Invernizzi, F. Bernuzzi, T. C. Lairmore, G. Alpini, and S. Glaser, Inhibition of microRNA-24 increases liver fibrosis by enhanced menin expression in Mdr2-/- mice, Journal of Surgical Research, 2017. Copyright © 2018 Copyright Clearance Center, Inc.

gene expression was increased in Mdr2$^{-/-}$ mice, BDL mice, and advanced stage human PSC samples. Treatment of Mdr2$^{-/-}$ mice with miR-24 VM increased menin expression, which correlated with increased expression of fibrotic genes. Mice treated with miR-24 VM showed significant increase in periductular fibrosis and bile duct mass. BDL mice treated with menin-MLL inhibitor displayed decreased hepatic damage, fibrosis, and intrahepatic biliary duct mass (IBDM). *In vitro,* inhibition of miR-24 significantly increased cholangiocyte expression of FN1, Col1α1, TGF-β1, and α-SMA. The menin/miR-24 regulatory system is implicated in cholestatic liver fibrosis. Inhibition of miR-24 increases menin and TGF-β1 expression, subsequently driving hepatic fibrosis and bile duct mass in Mdr2$^{-/-}$ mice, a murine model of PSC. We believe menin drives biliary proliferation and hepatic fibrosis in BDL mouse model through its interaction with MLL. Modulation of the menin/miR-24 and/or menin-MLL axis may provide novel targeted therapies to slow the progression of hepatic fibrosis into cirrhosis by altering TGF-β1 expression.

2.2 Introduction

Cholangiocytes represent 3-5% of cells within the liver and are the targets of cholangiopathies, such as PBC and PSC (36, 37). These cholangiopathies are characterized by the classical findings of cholestatic liver injury: increased number of biliary ductules, polymorphonuclear leukocyte infiltration, and the deposition of extra-cellular matrix that results in portal fibrosis and biliary cirrhosis (38). PSC, in particular, is characterized by chronic inflammation and obliterative fibrosis of the intra- and/or extra-hepatic biliary tree (39). This results in bile stasis and hepatic fibrosis that will progress to cirrhosis and the need for liver transplantation (39). PSC is also associated with a 5-10% lifetime risk for the development of CCA, 160-fold higher than the general population (40). Currently, medical therapies for PSC are limited to UCDA, and liver transplantation before the onset of end-stage liver disease remains the recommended treatment strategy (40, 41). More research regarding the cellular mechanisms behind cholangiocyte proliferation and portal fibrosis is needed in order to develop novel therapeutic strategies to mitigate disease progression.

Recently, menin was shown to exist in a negative regulatory feedback loop with miR-24 (42). miR-24 binds to the 3 untranslated regions of the MEN1 mRNA transcript to negatively regulate its protein expression. Menin, in turn, can positively regulate expression of miR-24 via MLL-driven histone trimethylation at both of miR-24 chromosomal locations, chromosome 9 and 19 (26). Overexpression of menin represses MEN1 promoter activity, indicating negative self-regulation. Increase in miR-24

expression is thought to be a possible mechanism driving MEN1 syndrome and thus targeting miR-24 expression is an attractive therapeutic possibility (43).

miR-24 activity is documented to drive both pancreatic and liver cancer, although its role in other tissues remains controversial (44, 45, 46). miR-24 is well documented to negatively regulate menin expression in the endocrine pancreas and drive tumorigenesis (42). There is strong evidence for the oncogenic role of miR-24 in PDAC as well. miR-24 overexpression was shown to decrease FZD5 (WNT receptor), HNF1B (HOX transcription factor), and TMEM92 to drive PDAC epithelial- mesenchymal-transition. A separate study showed that miR-24 regulated the BIM pathway to drive PDAC angiogenesis (45, 46). Melatonin negatively regulates miR-24 expression in several cancers to inhibit tumor proliferation and migration, and lower melatonin signaling in cholangiocytes leads to increased VEGF expression (47). MiR-24 expression is increased in HCC and its inhibition reduces proliferation, migration, and invasion (48).

In addition to miR-24, we used a small molecule inhibitor of the menin-MLL interaction to probe the role of menin in hepatic fibrosis. As mentioned earlier, the menin-MLL interaction recruits histone methyltransferases and opens chromatin conformation through transcription-activating histone trimethylation. The compound was initially designed to treat mixed-lineage leukemia (for which the MLL protein is named) in which genetic translocations result in a constitutively active MLL protein that actually requires the presence of menin in order to activate its target genes, thus facilitating leukemogenesis. MLL proteins have been linked to bile acid physiology, particularly

through their interaction with nuclear receptors and epigenetic control of bile acid transporter genes (49). However, menin-MLL role has not yet been investigated within the liver and it is unknown if mutant MLL-fusion proteins arise in liver pathophysiology.

TGF-β1 signaling and menin are well characterized in MEN1 syndrome. TGF-β1 binds TGF-β receptors to recruit SMAD proteins that translocate to the nucleus and activate transcription. It is shown in both the pituitary and parathyroid gland that menin physically interacts with Smad3 and drives expression of target genes (31). Loss of menin expression leads to uninhibited proliferation and ultimately carcinogenesis as seen in MEN1 syndrome. TGF-β1 signaling plays a prominent role in pancreatic physiology albeit its connection with menin is less understood. TGF-β1 signaling decreases proliferation in a number of pancreatic cell types: beta-cells (50), pancreatic stellate cells (51), and pancreatic ductal adenocarcinoma (PDAC) cells (52). Interestingly, a pancreatic-specific dominant negative TGF-β Receptor type II (dnTGFβrII) transgenic mouse exhibited less pancreatic fibrosis in response to injury (53). Thus, exploring the relationship between TGF- β1 and menin may help elucidate nuances between cellular proliferation and organ fibrosis.

TGF-β1 inhibits activation of quiescent hepatic stellate cells (HSC) via Smad7 activity but stimulates fibrotic reaction in activated HSCs or differentiated myofibroblasts via Smad3 activity (54). TGF-β1 is anti-proliferative and pro-apoptotic in hepatocytes (54). Loss of hepatic TGF-β signaling in dnTGFβrII mice is a model for primary biliary

cirrhosis (PBC) featuring anti- mitochondrial antibodies, lymphocytic infiltration, periportal fibrosis, and increased incidence of HCC (55). One study showed that dnTGFβrII mice displayed increased pro-inflammatory Treg cells compared to wild-type (WT) (56), indicating that TGF-β can affect non- parenchymal cell types.

Menin has been shown to interact with SMAD3 and the inactivation of menin blocks TGF-β1 signaling (33). SMAD3 phosphorylation and TGF-β1 have previously been shown to contribute to hepatic fibrosis (57); however, the role of menin in this pathway is unknown. The multidrug resistance gene-2 knockout (Mdr2$^{-/-}$) and bile-duct ligated (BDL) mouse is a widely utilized murine model of cholestatic liver disease that represents PSC and biliary obstruction, respectively, with characteristic biliary proliferation and portal fibrosis (57-59). We hypothesized that targeting menin expression/function could alter the progression of hepatic fibrosis.

2.3 Materials and Methods

All reagents were purchased from Sigma Aldrich (St. Louis, MO), unless otherwise indicated. Cell culture reagents and media components were purchased from Invitrogen Corporation (Carlsbad, CA). Total RNA and microRNA were isolated from cells and liver tissue using the mirVana miRNA isolation kit from ThermoFisher Scientific (Waltham, MA). Total RNA was used to create cDNA from 1200 μg of mRNA using iScript™ Reverse Transcription Supermix (Bio- Rad, Hercules, CA) for reverse transcriptase polymerase chain reaction (rtPCR). Primers for rtPCR were purchased from Qiagen (Valencia, CA), unless otherwise indicated. The rtPCR experiments were performed using SYBR Green PCR Master Mix from SABiosciences (Germantown, MD) on the Agilent Technologies Mx3005P rtPCR system.

MEN1 gene expression was quantified by rtPCR using RNA isolated from cultured mouse cholangiocytes, as well as mouse and human liver tissues. Fibrosis was evaluated by rtPCR using mouse primers for fibronectin 1 (FN1), type 1 collagen (COL1a1), TGF-β1 and alpha smooth muscle actin (α-SMA). Proliferation was evaluated by rtPCR using mouse primers for Ki-67 and proliferating cell nuclear antigen (PCNA). Glyceraldehyde-3-phosphate dehydrogenase (GAPDH) gene expression was used as a relative control. Data is expressed as relative mRNA levels.

In Vitro Studies

In vitro studies were performed using our immortalized murine cholangiocyte line (IMCL) (60), a gift from Dr. Yoshiyuki Ueno, Yamagata University, Yamagata, Japan. IMCL were cultured under standard conditions (5% CO2 and 37^{o}C incubation and treated with 75 nM of mirVana miR-24 inhibitor, mimic or the standard control for 24 hours, according to the manufacturers protocol. Cells were collected following treatment with Gibco®TrypLE dissociation reagent (Life Technologies, Grand Island, NY) and used for RNA isolation. Cholangiocyte and murine liver miR-24 expression was measured using rtPCR. Isolation of microRNAs was per- formed using the mirVana RNA isolation kit, with cDNA synthesized using the TaqMan^{TM} microRNA Reverse Transcription Kit from Applied Biosystems (Foster City, CA). Sequence specific primers for miR-24 and U6 control were purchased from Qiagen (Germantown, MD).

The luciferase assay was performed to determine if miR-24 directly interacts with the MEN1 gene to alter its expression in cholangiocytes. Luciferase constructs were obtained from Dr. Judy S. Crabtree (Louisiana State University, Baton Rouge, LA). These constructs consisted of a 1600-bp fragment of human MEN1 3-UTR cloned into a pmirGLO vector (pmirGLO-MEN1). A total of $5x10^5$ IMCLs per assay were co-transfected with pmirGLO-MEN1 at 5 pmol/0.5 mL medium. After 24 hr, luciferase levels were measured using Dual-Glo®Stop & Glo® per vendors instructions (Promega, Madison, WI), imaged using Thermo Scientific Varioskan Lux and analyzed using Thermo Scientific Skanit 4.1 software. Data are expressed as fold-change of firefly/renilla luminescence ± SEM.

Human Samples

Control and late stage PSC samples were obtained as a gift form Dr. Pietro Invernizzi, under a protocol approved by the ethics committee by the Humanitas Research Hospital (Rozzano, Italy) (57, 60). Total RNA was extracted from formalin-fixed, paraffin-embedded sections using the RNeasy® FFPE kit from Qiagen. Menin expression in control and late-stage PSC samples was verified using rtPCR.

In Vivo Studies

All animal experiments were performed according to protocols approved by the Baylor Scott & White Institutional Animal Care and Use Committee. Male FVB/NJ WT were purchased from The Jackson Laboratory (Sacramento, CA). The Mdr2$^{-/-}$ mouse colony is established in our facility. Animals were maintained in a temperature and light controlled environment with free access to drinking water and rodent chow. Male C57BL/6 (wild-type, WT, 12-week age, 25-30 gm) were purchased from Jackson Laboratory (Bar Harbor, ME), housed in a temperature- controlled environment (22C) with 12:12-hr light-dark cycles, fed standard rodent chow with free access at water ad libitum. WT mice were subject to either sham or BDL surgery for 7 days.

Inhibition of miR-24 signaling *in vivo* was performed using a miR-24 Vivo Morpholino purchased from Gene Tools, LLC. (Philomath, OR) (61). The miR-24 Vivo Morpholino sequence was 5-TCCTGTTCCTGCTGAACTGAGCCAG-3. Twelve-week-old Mdr2$^{-/-}$mice were treated with the miR-24 Vivo Morpholino (12.5 mg/kg) via tail vein

injection every other day for 1 week. Mice were euthanized and tissues were collected on the 7^{th} day following the first treatment. The menin-MLL inhibitor, MI-2-2, was purchased from EMD Millipore (Burlington, MA). WT sham and BDL mice were treated with vehicle or MI-2-2 (20-40 mg/kg, I.P.) for 1 week before collecting liver tissue.

Liver fibrosis was evaluated by Sirius Red staining in liver sections (5 μm thick) and by rtPCR of RNA isolated from total liver samples for the aforementioned genes associated with liver fibrosis. Bile duct mass was measured using IHC for cytokeratin-19 (CK-19), a cholangiocyte-specific protein (62). The tissues were stained with mouse polyclonal CK-19 antibody purchased from Abcam (Cambridge, MA) using a 1:200 dilution. The mouse IgG Vectastain® ABC Kit from Vector Laboratories, INC. (Burlingame, CA) was used for secondary staining. Light microscopy and IHC observations were taken with a BX-40 light microscope (Olympus, Tokyo, Japan). Semi-quantitative analysis was performed using Adobe Photoshop.

Statistical Analysis

All data are expressed as mean ± SEM. Differences between groups were analyzed by Students unpaired t-test when two groups were analyzed and ANOVA when more than two groups were analyzed, followed by an appropriate post-hoc test. $P<0.05$ was considered to be statistically significant.

2.4 Results

MEN1 Expression is Increased in Advanced Stage PSC and 66-week Mdr2$^{-/-}$ Mice

Expression of the MEN1 gene was measured by rtPCR in total liver tissues from FVB/NJ WT and Mdr2$^{-/-}$ mice at 12 and 66 weeks of age. MEN1 expression was significantly decreased in the 12-week old Mdr2$^{-/-}$ mice compared to the FVB/NJ control mice, but was significantly upregulated in the 66-week old Mdr2$^{-/-}$ mice (Figure 1A). This corresponded with increased expression of miR-24 at 12 weeks and decreased expression of miR-24 at 66 weeks in the Mdr2$^{-/-}$ mice (Figure 1B) compared to the FVB/NJ control mice. MEN1 expression measured in human liver from patients with advanced stage PSC was also upregulated, similar to the 66-week old Mdr2$^{-/-}$ mouse (Figures 1C-D). These data show that menin expression is variable throughout the lifespan of the Mdr2$^{-/-}$ mouse and is higher in mice with advanced disease.

miR-24 Regulates MEN1 Expression in Mouse Cholangiocytes

Inhibition of miR-24 in IMCLs corresponded with a significant increase in MEN1 gene expression (Figures 2A-B). Treatment of IMCLs with miR-24 mimic decreased MEN1 expression (Figures 2C-D). These results demonstrate that miR-24 participates in a negative feedback loop within cholangiocytes to alter the expression of menin. Results of the luciferase assay are shown in Figure 2E. Treatment of cholangiocytes with a miR-24 inhibitor significantly increased luminescence, whereas treatment with the miR-24 mimic significantly decreased luminescence. These results confirm that miR-24 directly interacts with the MEN1 gene to negatively regulate expression.

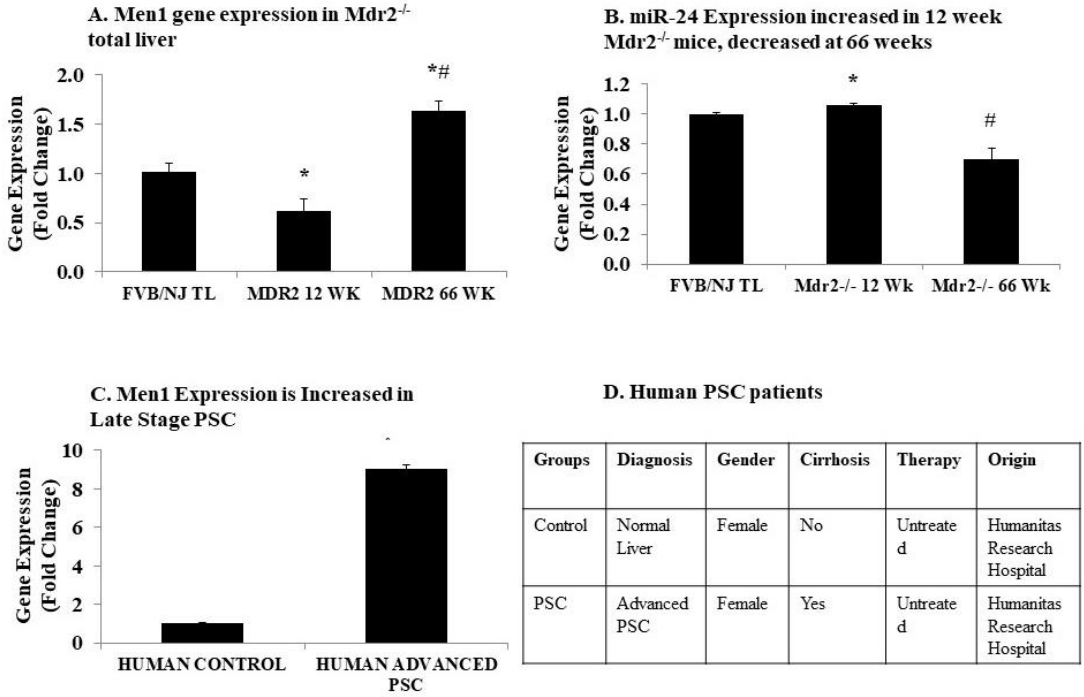

Groups	Diagnosis	Gender	Cirrhosis	Therapy	Origin
Control	Normal Liver	Female	No	Untreated	Humanitas Research Hospital
PSC	Advanced PSC	Female	Yes	Untreated	Humanitas Research Hospital

Figure 1: Men1 expression in Mdr2$^{-/-}$ mice.
A: Hepatic Men1 gene expression is decreased in 12-week Mdr2$^{-/-}$ mice and increased in 66-week Mdr2$^{-/-}$ mice compared to the FVB/NJ control mice when examined using rtPCR (n=3). B: Hepatic miR-24 expression is significantly increased in 12-week Mdr2$^{-/-}$ and decreased in 66-week Mdr2$^{-/-}$ compared to FVB/NJ control mice via rtPCR (n=3). C-D: Men1 gene expression is increased in human liver with advanced stage PSC compared to normal control liver (n=1). *$p \leq 0.05$ vs control.

Expression of MEN1 Correlates with Markers of Fibrosis

The expression of fibrotic genes was evaluated by rtPCR in IMCLs treated with a miR-24 inhibitor. When MEN1 expression was increased (Figure 2A), expression of FN1, COL1a1, TGF- β1, and α-SMA were also increased (Figure 3A). Inhibition of MEN1 with the miR-24 mimic resulted in decreased expression of these fibrotic genes (Figure 3B). These results demonstrate that the negative feedback loop between miR-24 and menin also contributes to the *in vitro* expression of genes associated with liver fibrosis.

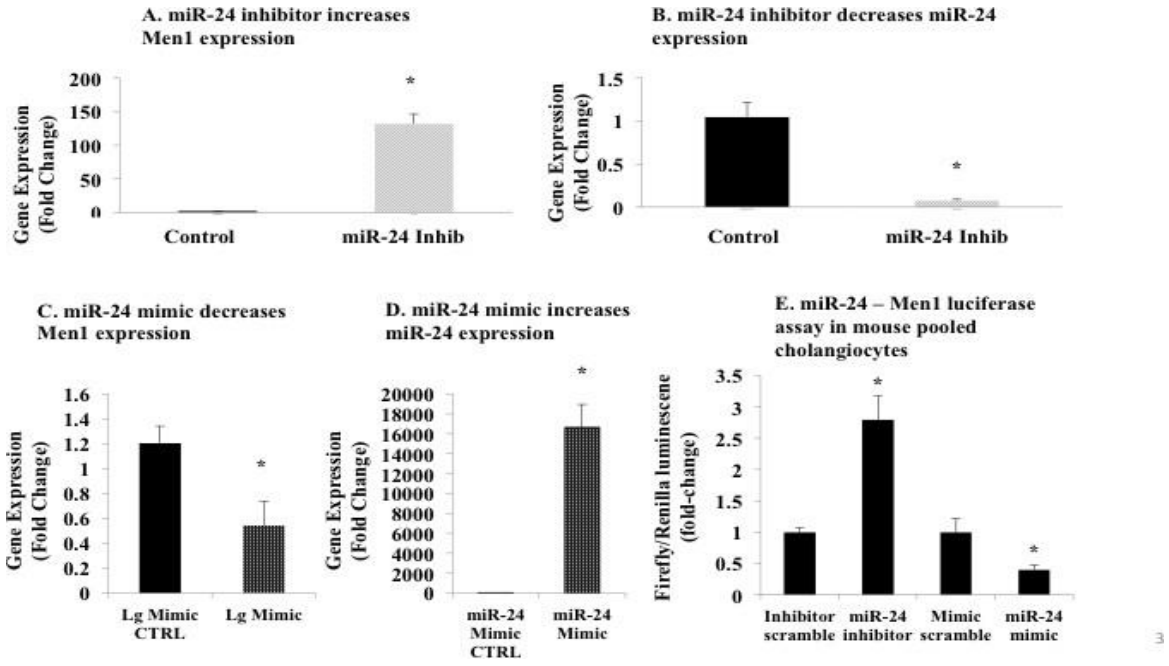

Figure 2: miR-24 negatively regulates Men1 expression
A-B: miR-24 inhibition increases Men1 expression and decreases miR-24 expression (n=3). C-D: miR-24 mimic decreases Men1 expression and increases miR-24 expression (n=3). E: miR-24 inhibition/mimic inversely alters luminescence of Men1 luciferase construct. (n=3). *$p \leq 0.05$ vs control.

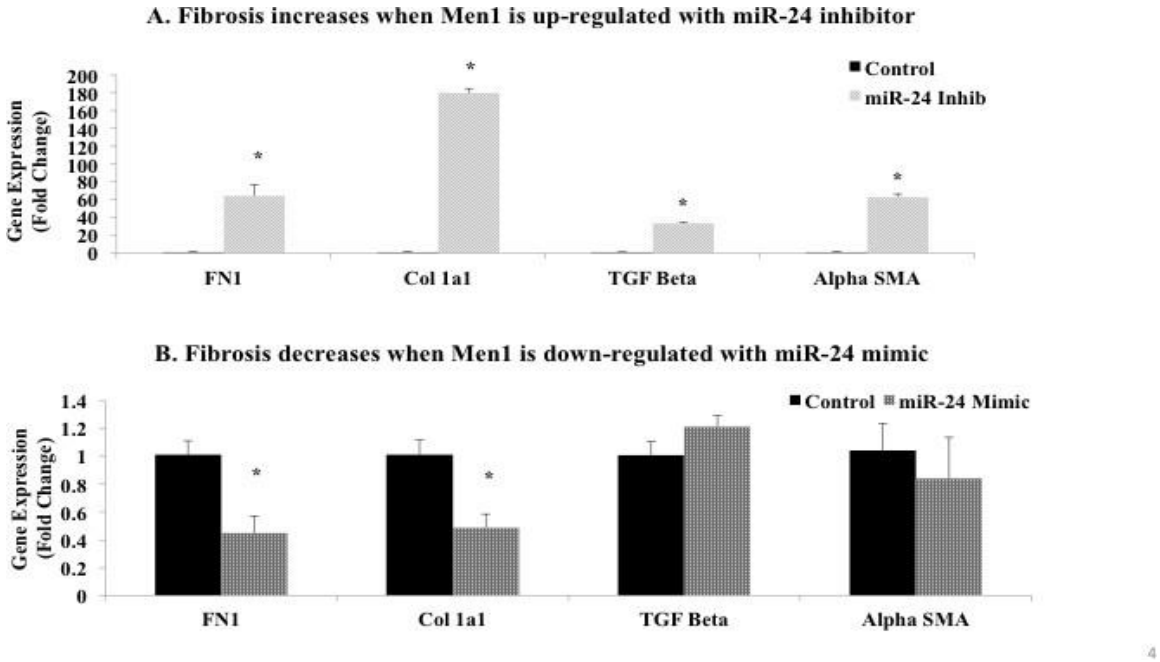

Figure 3: Men1 expression positively associates with expression of fibrotic markers.
A: Expression of fibrotic genes (FN1, Col 1a1, TGF-β1 and α-SMA) is increased in IMCL treated with miR-24 inhibitor (n=1). B: Expression of fibrotic genes (FN1 and Col 1a1) is decreased in mouse cholangiocytes treated with miR- 24 mimic. Expression of TGF-β1 and α-SMA did not significantly change with miR-24 mimic (n=1). *$p \leq 0.05$ vs control.

Inhibition of miR-24 in Vivo Regulates Expression of MEN1 and Drives Hepatic Fibrosis

Treatment of Mdr2$^{-/-}$ mice with miR-24 Vivo Morpholino significantly increased MEN1 expression in total liver tissues, as measured by rtPCR (Figure 4A). Expression of proliferation markers (Ki-67 and PCNA) did not significantly change with miR-24 Vivo Morpholino treatment (Figure 4B). Similar to our *in vitro* results, inhibition of miR-24 resulted in significantly increased expression of fibrotic genes, including TGF-β1 (Figure 4C). Sirius Red staining and semi-quantitative analysis of liver sections was performed to evaluate changes in hepatic fibrosis. Mdr2$^{-/-}$ mice treated with miR-24 Vivo Morpholino demonstrated significantly more collagen deposition than the FVB/NJ WT and untreated Mdr2$^{-/-}$ mice (Figure 5).

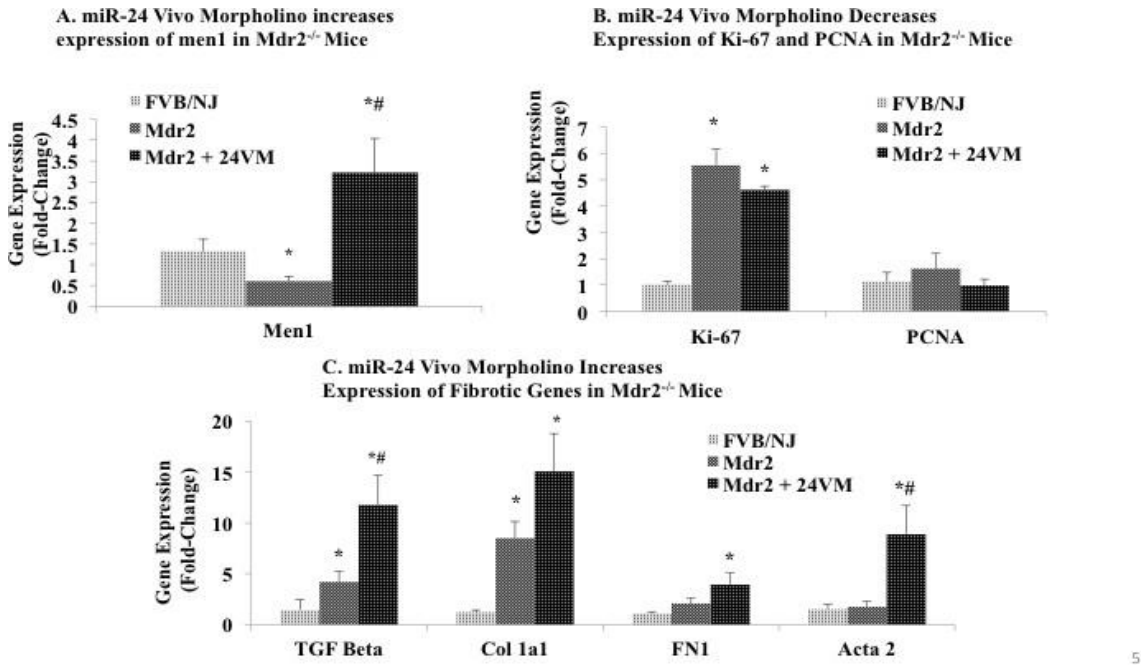

Figure 4: miR-24 vivo morpholino increases hepatic Men1 expression

A: Treatment of Mdr2$^{-/-}$ with miR-24 Vivo Morpholino significantly increases hepatic Men1 expression compared to mismatch scramble (n=3). B: Expression of proliferative markers do not significantly change. (n=3) C. Hepatic expression of fibrotic genes (FN1, Col1α1, TGF-β1, and α-SMA) increases in Mdr2$^{-/-}$ treated mice (n=3). *p$\leq$ 0.05 vs control.

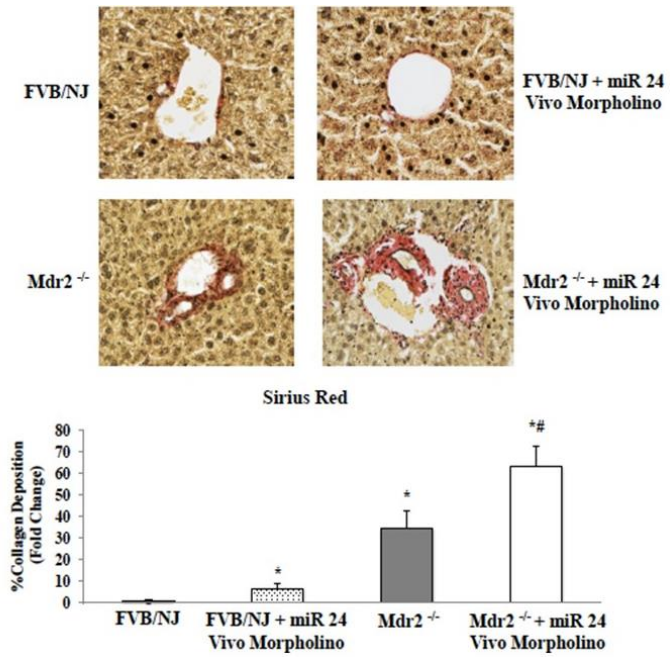

Figure 5: miR-24 vivo morpholino increases hepatic fibrosis in Mdr2$^{-/-}$ mice.

A: Sirius Red staining shows increased hepatic collagen deposition in Mdr2$^{-/-}$ mice treated with miR-24 Vivo Morpholino compared to untreated FVB/NJ and Mdr2$^{-/-}$ mice. *p $\leq$ 0.05 vs control.

Treatment of BDL Mice with M-2-2

Men1 gene expression is increased in total liver from BDL mice compared to WT (Figure 6A) but not in pure cholangiocytes (not shown). Treatment of BDL mice with MI-2-2 decreased focal hepatic necrosis and overall cellularity compared to untreated BDL via H&E staining (Figure 6B). IBDM decreased in MI-2-2 treated BDL mice compared to untreated BDL via CK-19 staining (Figure 7A-B). Hepatic fibrosis decreased in MI- 2-2 treated BDL mice compared to untreated via Sirius Red staining (Figure 8A-B).

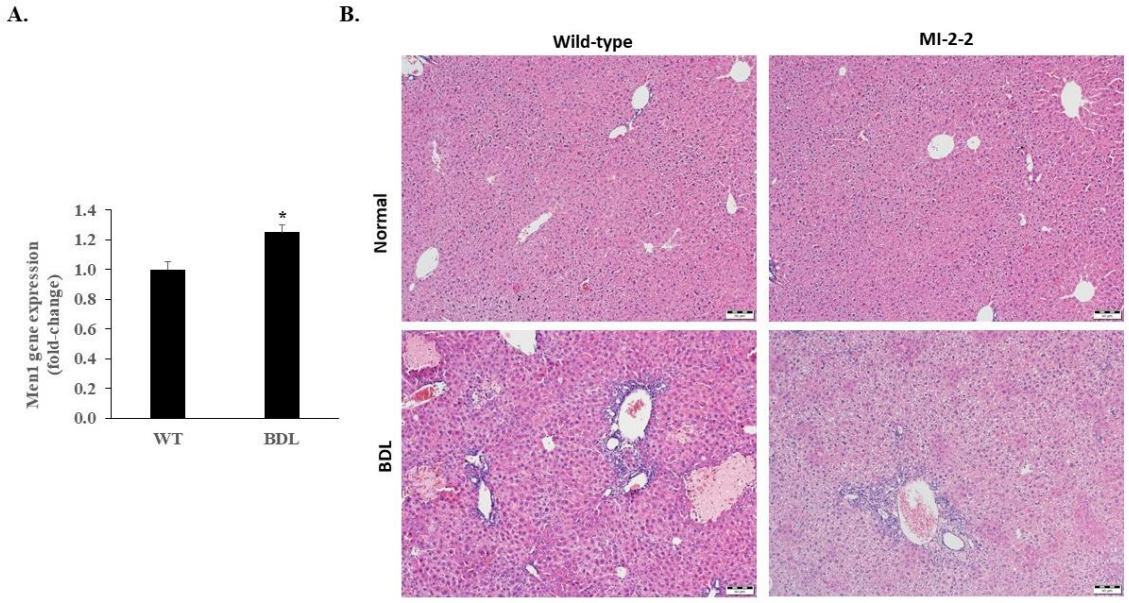

Figure 6: Menin-MLL interaction drives hepatic necrosis in BDL mice model.
A: Men1 gene expression increased in total liver (TL) following BDL but not pure cholangiocytes *p ≤ 0.05 vs control. B.: H&E staining shows sparing of focal hepatic necrosis in MI-2-2 treated BDL compared to untreated BDL.

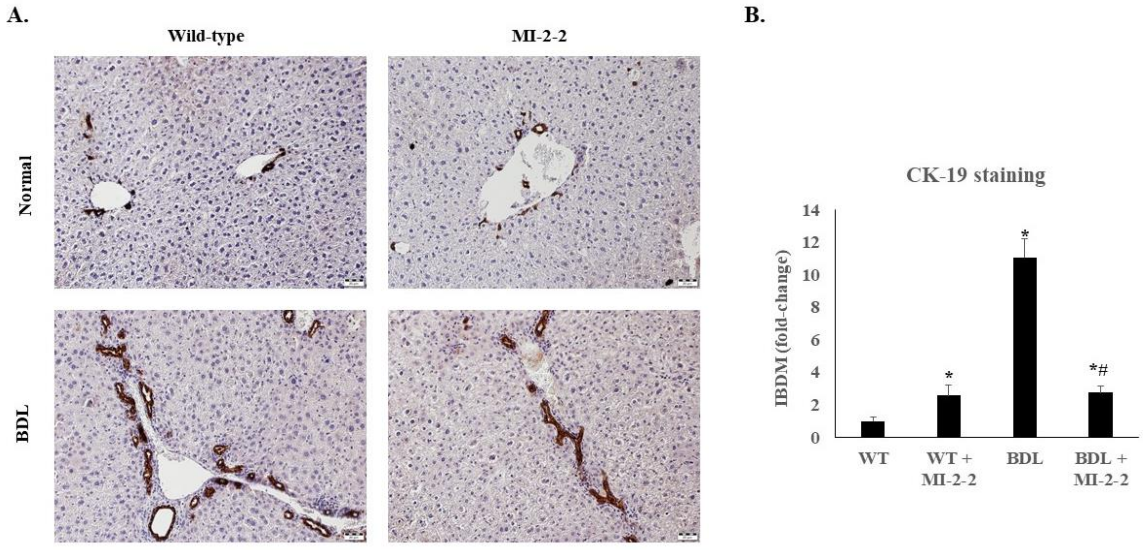

Figure 7: Menin-MLL interaction increases IBDM in BDL mice.
A-B: Ck- 19 staining shows decreased IBDM in MI-2-2 treated BDL compared to untreated BDL. *$p \leq 0.05$ vs WT, #$q \leq 0.05$ vs BDL.

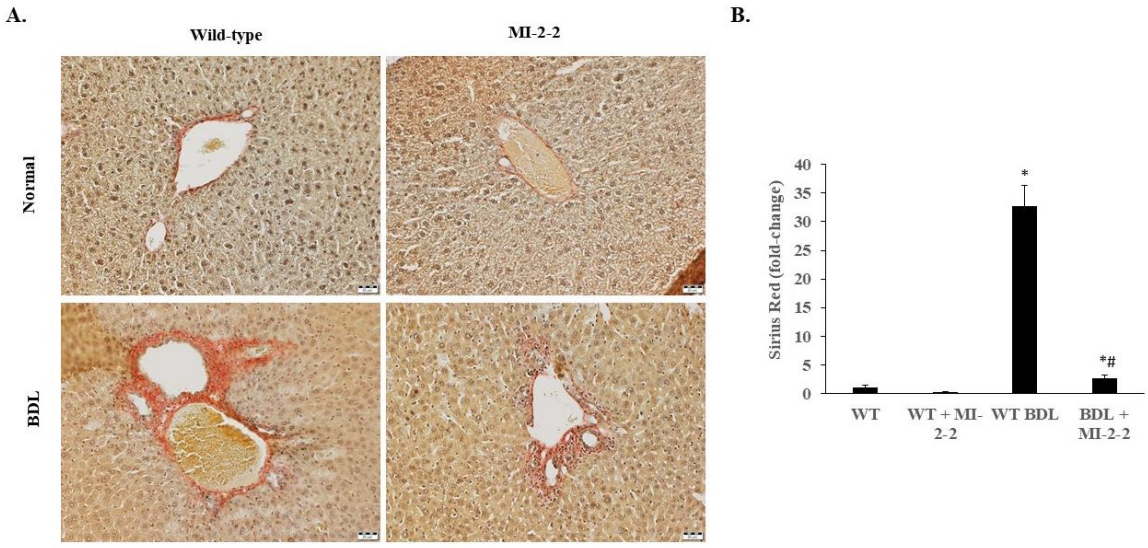

Figure 8: Menin-MLL interaction increases hepatic fibrosis in BDL mice.
A-B: Sirius Red staining shows decreased hepatic fibrosis in MI-2-2 treated BDL compared to untreated BDL. *$p \leq 0.05$ vs WT, #$q \leq 0.05$ vs BDL.

2.5 Discussion

The findings of this study suggest that the miR-24/menin regulatory system may play a key role in the progression of hepatic fibrosis. We demonstrated *in vitro* that miR-24 directly interacts with the MEN1 gene in murine cholangiocytes. Also, we demonstrated that inhibition of miR-24 signaling *in vitro* and *in vivo* increases MEN1 gene expression and subsequently promotes expression of fibrotic genes in cultured cholangiocytes and liver tissues, respectively. These findings correlate with increased MEN1 expression in patients with late stage PSC and the 66-week old $Mdr2^{-/-}$ mice. Furthermore, we have established that menin-MLL interaction drives biliary proliferation and hepatic fibrosis in BDL mouse model of cholestasis.

Menin has traditionally been characterized as a nuclear tumor suppressor protein due to its involvement in MEN1 syndrome, an autosomal dominant disorder characterized by tumors of the pituitary, parathyroid glands, and pancreatic islet cells [31]. Early studies suggested that menin inactivation contributes to parathyroid tumorigenesis through a loss of TGF-β1 signaling (35). Previous studies have also shown that menin interacts with SMAD3 to regulate TGF-β signaling (33). Specifically, inactivation of menin disrupts SMAD3 binding to its cognate DNA element and blocks TGF-β1 signaling (33). This pathway has been supported by other studies that suggest SMAD3 is also an important tumor suppressor that regulates menin and TGF-β1 signaling in parathyroid adenomas and pancreatic endocrine tumors (63, 64). Our study contributes to a small, but growing amount of evidence that suggests menin is involved in liver disease. We

have shown that upregulation of menin increases TGF-β1 expression and promotes fibrosis in cholangiocytes and in a murine model of cholestatic liver disease. Additional research in this model is needed to further elucidate menin's involvement and characterize the interactions between hepatocytes, cholangiocytes and HSCs.

Increased SMAD3/TGF-β1 signaling contributes to the development of hepatic fibrosis in cholestatic liver disease (57, 65), but menin's role in liver pathology has not been well defined. Zindy et al. demonstrated that MEN1 expression is upregulated in hepatocellular carcinoma (HCC) and in adjacent cirrhotic liver tissue (32 , 33). In this study, menin was a key regulator of hepatic fibrosis through TGF-β1 signaling and activation of hepatic stellate cells (32, 33). Xu et al. also demonstrated that menin expression is upregulated in HCC and expression correlates with a poor prognosis (66). Furthermore, a recent study by Cao et al. suggested that deletion of MEN1 in hepatocytes induced lipid accumulation and liver steatosis in aging mice (64).

This study also demonstrates that a negative feedback loop between miR-24 and menin exists within the liver and may play a role in the progression of liver disease. miR-24 has previously been shown to regulate menin expression within pancreatic islet cells, which affects the cells overall viability and proliferation (26). This negative feedback loop has also been demonstrated within parathyroid tissues and may contribute to the tumorigenesis of MEN1 syndrome (42). The interactions between miR-24, menin, and TGF-β1 have not been previously described, however, previous studies have reported a link between miR-24 and TGF-β1 signaling. Wang et al. demonstrated that miR-24

downregulates TGF-β1 signaling and mitigates cardiac fibrosis following myocardial infarction (67). Furthermore, miR-24 has been shown to decrease TGF-β1 signaling that results from mechanical stress (68).

While our studies focused on cholangiocytes, it is important to recognize the role that non-parenchymal cell types may play in cholestatic disease states. Inhibiting miR-24 expression or menin-MLL interaction can have a profound effect on macrophage maturation and polarization. MLL-dependent H3K4-me3 and H3K27 demethylation characterize pro-inflammatory M1 polarization while alternative M2 polarization is characterized by DNA methyltransferase and histone deacetylase. M1 macrophages that were treated with a menin-MLL inhibitor exhibited decreased expression of the proinflammatory cytokine CXCL10 (69). Interestingly, the M2 macrophage phenotype is more prevalent in CCA tissue and is associated with secretion of factors that suppress immunity and facilitate CCA angiogenesis and EMT activity (70). However, miR-24 activity was shown to suppress cytokine production and M1-type pro-inflammatory differentiation of macrophages (71).

As a ubiquitously expressed protein, menin plays a role in immune cells. Recently, menin has been implicated in CD4+ T cell immunosenescence and the senescence-associated secretory phenotype (72). Senescent CD4+ T cells exhibit irregular homeostasis and cytokine production that can contribute to cancer, infectious disease, and autoimmune disease (72). Menin binds to the BACH2 locus and suppresses its expression through histone deacetylation. Decreased BACH2 expression increases

cellular senescence. The role of menin in immune cells and hepatobiliary diseases such as PSC, PBC and cholangiocarcinoma has not been explored.

Th17+ T cell differentiation is menin-dependent as well. In naive CD4+ T cells, menin is recruited to the IL17 locus to drive its expression. Furthermore, menin binds the RORC locus to drive expression of ROR$\gamma\delta$ in order to maintain Th17+ T cell differentiation and function (73). IL17 secretion by Th17+ T cells can trigger HSC activation, collagen deposition, and subsequent hepatic fibrosis (74). Peripheral blood mononuclear cells from patients with PSC showed a significantly higher proportion of Th17+ cells compared to healthy patients (75). In MDR2$^{-/-}$ mice, the prevalence of IL-17+CD4+ T cells is thought to come at the expense of anti-inflammatory Foxp3+ regulatory T cells (76, 77, 78). Interestingly, Foxp3 interacts with EZH2, a polycomb group protein and menin-binding partner involved in chromatin silencing, to suppress gene expression through DNA and histone methylation. Ezh2$^{-/-}$ T cells failed to adequately differentiate into Foxp3+ regulatory T cells nor function properly *in vivo* (79). Thus, targeting menin expression in Th17+ or nave CD4+ T cells could ameliorate the fibrotic reaction in cholestatic liver disease.

Inhibiting menin expression also seems to decrease effector antigen-specific CD8+ T cells, which were shown to be pro-fibrotic in a bile-duct ligated mouse model of cholestasis (77) (80). Yamada et al. infected CD8+ T cell-specific menin knockout mice with Listeria monocytogenes ovalbumin-expressing bacteria in order to assess menin's role in the antigen-specific CD8+ T cell response. The lack of CD8+ T cell menin

expression reduced cell proliferation and survival upon infection via induction of cell cycle inhibitors, proapoptotic genes, and transcription factors associated with effector CD8+ T cell death (80). Thus, theoretically, overexpressing menin could drive proliferation and survival of effector CD8+ T cells necessary to clear infection but provoke hepatic fibrosis as a consequence.

While menin expression is directly implicated in CD4+ T cell senescence, Th17+ T cell differentiation and maintenance, and CD8+ effector T cell survival, it is indirectly implicated in CD4+ Th2 cell development through the MLL complex (81). $MLL^{+/-}$ cells were able to differentiate into Th2 memory cells but not able to maintain H3K4-methylation and H3K9-acetylation at the Th2 and GATA loci nor expression of Th2 cytokines IL-4, IL-5, and IL-13 (81). Later studies showed that co-immunoprecipitated Menin and MLL from the c-Myb/GATA-2 complex is necessary for Th2 memory cell formation (82). Interestingly, menin was more prevalent at the GATA-3 promoter site under Th2-promoting conditions, while MLL was more prevalent among CD4+ effector/memory cells. Enhanced Th2 activity has been implicated in IG4-related cholangitis (83). However, overall measurements of Th1/Th2 ratios in PSC/PBC populations have been inconsistent (84). Currently, there is limited research on the expression profile of miR-24 and menin-MLL interaction in liver disease. It has been shown that miR-24 is downregulated in cholangiocytes isolated from a rat model of polycystic liver disease (85). One study has also shown that miR- 24 is downregulated in a model of acute cholestatic hepatitis produced by alpha-naphthylisothiocyanate administration (86). Our study suggests that using miR-24 to downregulate menin and

TGF-β1 signaling may also have a therapeutic affect within the liver; however, additional studies are needed to support this hypothesis. With more research, miR-24 may be added to the growing list of microRNAs (miR-29, miR-21, miR-122) that provide a therapeutic benefit by mitigating the progression of liver fibrosis (87).

The role of miR-24 and menin-MLL interaction in the progression of liver disease that we present in this study is a novel concept with therapeutic potential, but we must consider the limitations of the study. The amount of human data in this study is low due to the limited availability of human tissues. The Mdr2$^{-/-}$ mouse is a valid model of cholestatic liver disease, but additional studies with human tissues are necessary to explore expression patterns and signaling pathways of miR-24 and menin throughout the progression of cholangiopathies, such as PSC and PBC. Furthermore, we have shown that inhibition of miR-24 increases menin expression and drives hepatic fibrosis. The therapeutic potential of this pathway may involve upregulating miR-24 expression or inhibiting menin-MLL function. This could involve the delivery of miR-24 to liver tissues or the systemic administration of a menin-MLL inhibitor (88). Additionally, we need to consider other models of liver disease, such as alcohol-induced cirrhosis, non-alcoholic steatohepatitis, and viral-induced hepatitis, to determine whether or not other types of liver disease may benefit from targeting this pathway. In conclusion, the miR-24/menin regulatory axis and the menin-MLL interaction regulates TGF-β1 and the progression of hepatic fibrosis in Mdr2$^{-/-}$ and BDL mice respectively. This pathway has not been previously described within hepatology literature and has therapeutic potential for the management of cholestatic liver diseases, such as PSC and PBC.

3. MENIN ACTS AS A TUMOR SUPPRESSOR IN CHOLANGIOCARCINOMA [3]

3.1 Overview

Menin (MEN1) is a tumor suppressor protein in neuroendocrine tissue. Since cholangiocytes can take on a neuroendocrine phenotype, we tested the novel hypothesis that menin regulates cholangiocarcinoma proliferation. Menin and miR- 24 expression levels were measured in the following intra- and extrahepatic CCA cell lines: Mz-ChA-1, TFK-1, SG231, CCLP, HuCCT-1, and HuH-28, as well as the non-malignant human intrahepatic biliary line, H69. miR-24 miRNA and menin protein levels were manipulated *in vitro* Mz-ChA-1 cell lines. Markers of proliferation and angiogenesis (Ki67, VEGFA/C, Tie1/2, VEGFR-2/3 & Ang1/2) were evaluated. Invasion and migration were evaluated with Boyden chamber and scratch assays. Mz-ChA-1 cells were injected into the flanks of nude mice and treated with miR-24 inhibitor or inhibitor scramble. Menin expression was decreased in advanced CCA specimen while miR-24 expression was increased in CCA. Menin overexpression decreased proliferation, angiogenesis, migration, and invasion. Inhibition of miR-24 increased menin protein expression while decreasing proliferation, angiogenesis, migration, and invasion. miR-24 was shown to negatively regulate menin expression by luciferase assay. Tumor burden and expression of proliferative and angiogenic markers was decreased in the miR-24 inhibited tumor group compared to controls. Interestingly, treated tumors were more fibrotic then the control group. miR-24-dependent expression of menin may be important in the regulation of non-malignant and CCA proliferation and may be an additional therapeutic tool for managing CCA progression.

[3] § Part of this chapter is reprinted with permission from L. Ehrlich, C. Hall, J. Venter, D. Dostal, F. Bernuzzi, P. Invernizzi, F. Meng, J. P. Trzeciakowski, T. Zhou, H. Standeford et al., miR-24 inhibition increases menin expression and decreases cholangiocarcinoma proliferation, The American Journal of Pathology, vol. 187, no. 3, pp. 570580, 2017. Copyright © 2018 Copyright Clearance Center, Inc

.

3.2 Introduction

CCA is a biliary epithelial adenocarcinoma associated with late diagnosis, poor long-term survival, and limited responsiveness to current therapies (89). The topographical range of biliary histology contributes to the heterogeneous presentation of CCA, although its classification as intra- or extra-hepatic remains to be anatomically based (90). Cholangiocytes proliferate in response to damage and various endothelial stressors. During cell proliferation, cholangiocytes adopt a neuroendocrine-like phenotype via autocrine/paracrine signaling by cytokines (interleukin-6), vascular growth factors (VEGF) and neuropeptides (91, 92). Surgery is potentially curative for early disease, but few patients are surgical candidates and 5-year survival rates remain low (89, 90). Clearly, there is a need for advanced diagnostic strategies and improved targeted therapies for CCA.

Menin, encoded by the MEN1 (multiple endocrine neoplasia type I) tumor suppressor gene, is a 610 amino acid, 67 kilodalton nuclear protein that is ubiquitously expressed in all tissues and evolutionarily conserved, but shares little sequence homology with other proteins (17). Although menin's function has not been comprehensively elucidated, several studies have suggested that it is a scaffold protein involved in diverse cell functions including binding and regulating transcription factor activity (93), modifying histone proteins and chromatin structure (94, 95), and DNA repair (96, 97, 98). Loss of heterozygosity at the MEN1 gene locus (11q13) inactivates or deletes menin leading to tumorigenesis. Patients with MEN1 syndrome develop parathyroid

neoplasms (95%), gastro-entero-pancreatic tract neuroendocrine tumors (40%), and pituitary adenomas (30%) as well as tumors in non-endocrine tissues such as lipomas and cutaneous angiofibromas (99%).

Since menin's discovery as a tumor suppressor protein in MEN1 syndrome, it has been shown to regulate cell proliferation in lung, stomach, liver, breast, and prostate tissue (27, 28, 29, 99, 100); however, menin's role in liver carcinogenesis has not been widely studied. One study has shown that menin expression is downregulated in HCC, and that overexpressing menin *in vitro* decreased cell proliferation and gene expression of inflammatory cytokines (29). However, another study has shown that menin is upregulated in HCC samples and promotes HCC formation via interaction with MLL histone methyltransferase complex and overexpression of homeobox A (HOXA) genes (66). While menin appears to play a role in HCC formation, its role in CCA development and progression has not been studied.

Recent evidence demonstrates that menin and miR-24 form a negative regulatory feedback network to tightly control cell cycle and apoptotic genes (26, 42). MiR-24 targets menin's 3'-UTR, resulting in decreased menin protein expression. Conversely, Vijayaraghavan et al. showed that the menin-MLL protein complex is present upstream of miR-24 in both of its chromosome locations and that over-expression of menin increases miR-24 expression (26). MiR-24 has been implicated as an oncogene in a host of other cancers, particularly in the gastrointestinal tract (101-104).

We propose that menin and miR-24 contribute to a regulatory negative-feedback loop that maintains cholangiocyte proliferation and that dysregulation leads to malignant growth. We have demonstrated the novel finding that menin is downregulated in human CCA cell lines and advanced stage human CCA samples and modulation of menin expression alters cholangiocarcinoma proliferation. We have also shown that miR-24 expression is upregulated in human CCA cell lines and human CCA samples and modulation of miR-24 expression alters cholangiocarcinoma proliferation through changes in menin expression.

3.3 Materials and Methods

Materials

Reagents were purchased from Sigma (St. Louis, MO), unless otherwise indicated. Human MEN1 siRNA (sc-35922) (Santa Cruz Biotechnology) and control vectors were purchased from Santa Cruz Biotechnology (Dallas, TX). Human pCMV6-Entry MEN1 cDNA and control vector were purchased from Origene (Rockville, MD) and transfected with Lipofectamine® 2000 Transfection reagent (Thermo Fisher Scientific, Grand Island, NY). miRIDIAN microRNA Human hsa-miR-24-1 5p mimic (C-300495-07-0005), hairpin inhibitor (IH-300495-08-0005), and negative controls were purchased from GE Dharmacon (Lafayette, CO) and were transfected with Lipofectamine® RNAiMAX Transfection reagent (ThermoFisher Scientific). The RNeasy Mini Kit for RNA purification and all the following primers were purchased from Qiagen (Valencia, CA): Menin (MEN1, NM_000244); Glyceraldehyde-3-phosphate dehydrogenase (GAPDH, NM_002046); MKI67(NM_001145966); VEGF-A (NM_001025366); VEGF-C (NM_005429); VEGFR-2(NM_VEGFR-2); VEGFR-3 (NM_002020); ANG-1 (NM_001146); ANG-2 (NM_001118887); TIE-1 (NM_001253357); TIE-2 (NM_000459).

Antibodies used were as follows: hsa-miR-24-1 (002440 Taqman® ThermoFisher Scientific), U6 snRNA (004394 Taqman®), Menin (A300-105A, Bethyl Laboratories, Montgomery, TX), Ck-19 (Ab15463 (Abcam, Cambridge, MA), Ki67 (Ab15580, Abcam), and CD31 (89C2, Cell Signaling Technology, Danvers, MA).

Cell Lines

We studied six human CCA cell lines: Mz-ChA-1, TFK-1, SG231, CCLP-1, HuCC- T1, and HuH-28. The human intrahepatic CCA cell lines CCLP-1 (105), HuCC- T1 (106), and SG231 (107) were a gift of Dr. A. J. Demetris of University of Pittsburgh (Pittsburgh, PA). The human extrahepatic CCA line, Mz-ChA-1 (108), was a gift from Dr. G. Fitz (UT Southwestern Medical Center, Dallas, TX). The human intrahepatic biliary cell line, HuH-28 (109) and the human extrahepatic biliary TFK-1 cells (110) were obtained from the Cancer Cell Repository (Tohoku University, Japan); the cell lines were maintained as described (111). The human immortalized, nonmalignant, cholangiocyte cell line, H69, was obtained from Dr. G. J. Gores of Mayo Clinic, (Minneapolis, MN) (112).

Expression of Menin in Nonmalignant and CCA Cells and cDNAs from Control and CCA patients

Real-time PCR analysis of H69 and all CCA cell lines was evaluated using 1 g of RNA (113). Glyceraldehyde-3-phosphate dehydrogenase was used as a control primer along with the SYBR Green real-time PCR kit (SABiosciences, Frederick, MD). A $\Delta\Delta$Ct (delta delta of the threshold cycle) analysis was performed using H69 as the control sample (114). Data are expressed as relative mRNA levels ± SEM (n = 3).

We evaluated the expression of MEN1 mRNA in cDNAs obtained from three control patients and three CCA patients (Figure 13C); these samples were obtained from Dr. Pietro Invernizzi (Humanitas Research Hospital, Rozzano, Italy) under a protocol number approved by the Ethics Committee of by the Humanitas Research Hospital; the

protocol was also reviewed by the Veterans Administration Institutional Review Board (Temple, TX) and Research & Development Committee. The use of human tissue was also approved by the Texas A&M Health Science Center College of Medicine Institutional Review Board (College Station, TX). Real-time PCR was performed in triplicate.

For immunoblotting analysis (115), protein was obtained and quantified from whole cell lysates from nonmalignant and CCA cell lines and 40 μg was loaded into each well. Blots were blocked overnight and then stained with menin antibody at a 1:2000 dilution and β-actin antibody at a 1:5000 dilution. Data are expressed as fold change (mean ± SEM (n = 3)) of the relative expression after normalization with β-actin (housekeeper).

Measurement of menin expression was also performed using flow cytometry as described (115). Briefly, H69 and Mz-ChA-1 cells (the CCA lines implanted into athymic mice) were harvested from culture plates using TrypLE™ solution (ThermoFisher Scientific, Grand Island, NY), and washed with appropriate dilution of fixation buffer (eBioscience, Inc., San Diego, CA). Cells were resuspended at a minimum of $5x10^5$ cells/mL in 1x permeabilization buffer (eBioscience, Inc.) and incubated for 15 minutes at room temperature with menin antibody at a dilution of 1:100. Then Alexa Fluor® 488 conjugated secondary antibody was added to suspension at a dilution of 1:50 and cells were incubated for 15 minutes at room temperature in the dark. Cells incubated without antibody or with only Alexa Fluor® 488 conjugated secondary

antibody were used as negative controls. Cells were analyzed using (FACSCalibur, Becton Dickinson, San Jose, CA), with CellQuest Pro 5.2 software. At least 10,000 events in the light scatter (SSC/FSC) were acquired. The expression of menin was identified and gated on FL1-A/count plots. The relative quantity of the selected proteins (mean selected protein fluorescence intensity) is expressed as mean FL1-A (samples)/mean FL1-A (secondary antibodies only) (n=3).

Modulation of Menin Expression, Proliferation and Angiogenesis in Vitro

Mz-ChA-1 cells were targeted for the transient knockdown of menin expression using a human MEN1 siRNA (Santa Cruz Biotechnology) (sc-35922) along with siRNA Transfection Reagent (Santa Cruz Biotechnology) (sc-29528) according to the vendor's instructions. Mz-ChA- 1 cells were targeted for menin overexpression using the pCMV6-Entry expression vector containing MEN1 cDNA purchased from Origene (Rockville, MD) (113) and the Lipofectamine® 2000 Transfection reagent (ThermoFisher Scientific,) according to manufacturer's protocol. Transfected cell lines were allowed to grow for 24-48 hours before harvesting.

The menin-containing plasmid was amplified using ElectroMAX™ DH5-DH™ Competent Cells (Qiagen) and Invitrogen imMedia™ CITE™ agar and liquid media and isolated using Qiagen mini kit according to vendor's instructions. Plasmid yields were quantified using ND-1000 NanoDrop (ThermoFisher Scientific). The pCMV6-Entry vector without the Men1 insert was used as a control.

Transfection efficacy was assessed by measuring menin expression by real-time qPCR and flow cytometry (114) (116). Cell proliferation was measured by Ki67 real-time PCR expression, migration via wound healing (117), invasion via Boyden chamber, and angiogenesis via VEGF- A, VEGF-C, VEGFR-2, VEGFR-3, ANG- 1, ANG-2, TIE-1, and TIE-2 real-time PCR expression.

Wound Healing Assay

Mz-ChA-1 cells were plated on 6-well plates as described above and transfected 24 hours later. Twenty-four hours post-transfection, cells were tryspinized and reseeded on a new 6- well plate with twice the number of cells. Twenty-four hours later, a wound was initiated in the cell monolayer using a small pipette tip and a 19 gauge needle (117). Phase contrast images were taken at 0, 3, 6, 24, and 48 hours with a Nikon Eclipse TS100 microscope and NIS-elements D 4.00.07 soft- ware was used to measure the width of the wound (Nikon, Melville, NY). Data are expressed as fold-change of relative widths compared with 0 hour measurements of their respective transfected cell type ± SEM (n = 6). Statistical significance was valuated between control and transfected cell types at respective time points.

Boyden Chamber Migration Assay

Migration of Mz-ChA-1 cells was evaluated using QCM CITETM ECMatrix Cell Invasion Assay (Millipore, Billerica, Massachusetts) according to manufacturer's protocol. Fluorescence was read at 480/520 nm using a VersaMax microplate reader. Data are expressed as fold-change of transfected cell lines relative to control cell

lines± SEM (n = 7).

Proliferation Assay

Cell proliferation was measured by the CellTiter 96™ Aqueous Non-radioactive cell proliferation assay (Promega, Madison, WI) (113). Absorbance was measured at 490 nm on a microplate spectrophotometer (VersaMax, Molecular Devices, Sunny- vale, CA). Data were expressed as the degree of change of treated cells compared with vehicle-treated controls (n=7). Proliferation assay was used to assess the effects of altered Men1 and miR-24 expression on CCA cell growth.

Expression of miR-24 in Nonmalignant and CCA Cells and miRNA Sequencing Data from Control and CCA Patients

MiRNA was isolated from samples using the Ambion mirVana™ miRNA isolation kit per protocol [113]. cDNA libraries were created using TaqMan® microRNA RT kit per protocol (ThermoFisher Scientific) a TaqMan® MicroRNA Assay hsa-miR-24 primers. (ThermoFisher Scientific). TaqMan Universal PCR Master mix was used for real-time PCR, and U6 snRNA were used for endogenous control (ThermoFisher Scientific). A $\Delta\Delta$Ct (delta delta of the threshold cycle) analysis was performed using normal H69 as controls. Data are expressed as fold-change of relative microRNA levels ± SEM (n = 3).

MiRNA-sequencing data was obtained from nine human CCA patients from the Cancer

Genome Atlas Research Network (http://cancergenome.nih.gov, last accessed April 7, 2016) via the Genomic Data Commons Data Portal the Cancer Genome Atlas -CHOL. File manipulation was performed with Python, Python Software Foundation, Python Language Reference, version 2.7. (http://www.python.orglast accessed April 7, 2016). Example coding for this process can be found at https://github.com/ehrl1ch/RNA-Seq (last accessed April 7, 2016). MiR-24 expression is displayed as normalized miRNA transcripts count for each tumor sample compared with its matched human control. A t-test was performed to assess statistical significance.

Luciferase Construct

Experiments were performed to test whether mir-24 directly interacts with menin to change its expression. Luciferase constructs were obtained from Dr. Judy S. Crabtree (Louisiana State University, Baton Rouge, LA). These constructs consisted of a 1600-bp fragment of human MEN1 3-untranslated region cloned into a pmirGLO vector (pmirGLO-MEN1). The plasmid was amplified and isolated according to the protocol described above. A total of $5x10^5$ Mz-ChA-1 cells per assay were co-transfected using techniques described above with pmirGLO-MEN1 at 0.5 µg/well along with miR-24-1 mimic or hairpin inhibitor in addition to negative control at the concentration of 5 pmol/0.5 ml medium. After 24 hr, luciferase levels were measured using Dual-Glo®Stop & Glo® per vendors instructions (Promega, Madison, WI), imaged using Thermo Scientific Varioskan Lux and analyzed using Thermo Scientific Skanit 4.1 software. Data are expressed as fold-change of firefly/renilla luminescence ± SEM (n = 3).

Modulation of miR-24 in Vitro

We next performed experiments to determine whether miR-24 changes in Mz-ChA-1 cells lead to changes in menin expression and subsequently CCA proliferation. Mz-ChA-1 cells were targeted for miR24 knockdown using miR-24 hairpin inhibitor (GE Dharmacon, IH-300495-08-0005) using the Lipofectamine® RNAiMAX Transfection reagent (ThermoFisher Scientific, Grand Island, NY) according to the vendors instructions. After 24-48 hours, cells were harvested and transfection efficiency was assessed by measuring miR-24 TaqMan® microRNA expression. Menin protein expression was assessed using FACS. Cells were also assessed for proliferation via MTS assay, migration via wound healing (117), invasion via Boyden chamber, and expression of Ki67 and angiogenic factors were determined using real-time PCR.

In Vivo Studies

Male BALB/c eight-week-old nude (nu/nu) mice were kept in a temperature- and light-controlled environment with free access to drinking water and rodent chow (118). Mz-ChA-1 cells were suspended in extracellular matrix gel and subcutaneously injected into the left rear flanks of these nude mice. The experimental group received miR-24 hairpin inhibitor (GE Dharmacon, IH-300495-08-0005) injected directly into tumor at 4 ng/mm^3 three times per week, whereas the control group received a hairpin inhibitor scramble. Tumor growth was measured three times a week using an electronic caliper, and volume was determined as follows: tumor volume (mm^3) = π/6 x length (mm) x width (mm) x height (mm). Tumors were allowed to grow until the maximum allowable tumor burden was

reached, as set forth by the Baylor Scott & White Healthcare Institutional Animal Care and Use Committee tumor burden policy (http://researchers.sw.org/imedris/imedris), last accessed April 7, 2016). After 8 weeks, mice were euthanized with sodium pentobarbital (50 mg/kg body weight i.p.). We evaluated biliary proliferation in CCA tumor sections via immunohistochemistry (IHC) for CK-19, a cholangiocyte-specific marker, Ki67, and Sirius Red, a collagen-specific dye. In CCA tumor tissue, we measured the expression of menin, biliary proliferation (by real-time PCR for Ki67), and the expression of select angiogenic factors (CD31).

Statistical Analysis

All data are expressed as means ± SEM. Differences between groups were analyzed by Students unpaired t-test when two groups were analyzed and ANOVA when more than two groups were analyzed, followed by an appropriate post hoc test.

3.4 Results

The Expression of Menin is Decreased in CCA

By real-time PCR and immunoblots, we demonstrated that MEN1 mRNA and protein expression was significantly decreased in all selected CCA lines compared to H69 cells (Figure 9A-B). Similarly, by flow cytometry we demonstrated that menin expression was decreased in Mz-ChA- 1 cells compared to H69 cells (Figure 9C). By real-time PCR, there was reduced mRNA expression of menin in samples from human biopsies from patients with advanced grade CCA compared to control non- malignant samples (Figure 9D).

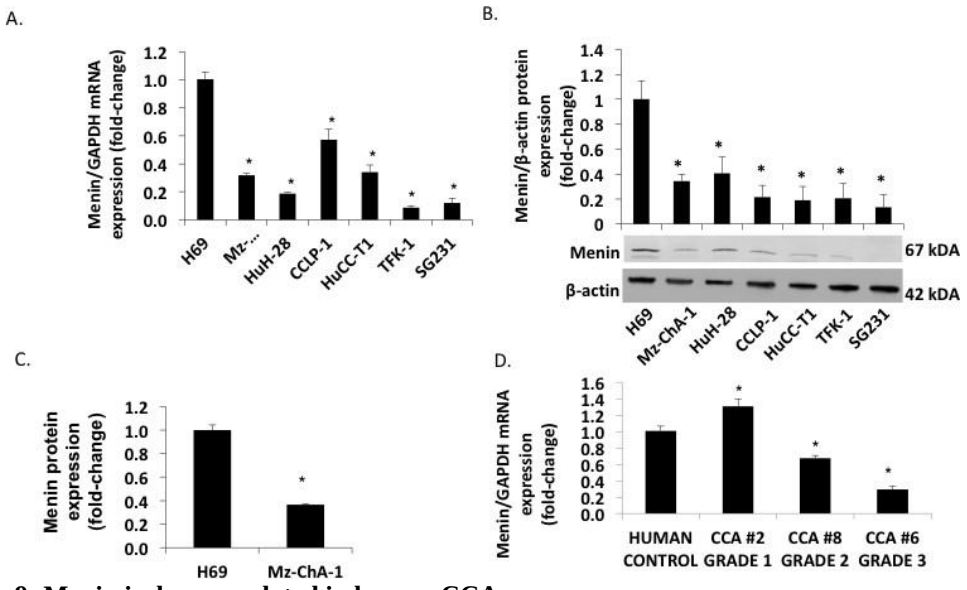

Figure 9: Menin is downregulated in human CCA.
A-B: Menin expression is decreased in CCA cell lines by rtPCR and immunoblots, respectively (n=3). C. Menin expression is decreased in Mz-ChA-1 cell line, via flow cytometry. D. Menin expression is decreased in advanced stage human CCA tissue biopsies compared with normal control. *$p \leq 0.05$ vs H69.

Menin Regulates CCA Cell Growth

To evaluate the role of menin in the regulation of CCA proliferation, we manipulated menin expression in Mz-ChA-1 cells. Menin expression was first decreased by MEN1 siRNA in Mz-ChA-1 cells (Figure 10A-B). Based on nuclear Ki67 protein expression, menin knockdown resulted in increased Mz-ChA-1 cell proliferation compared to controls (Figure 10C). In contrast, overexpression of menin, by transfection with a pCMV6-Entry vector containing the MEN1 gene insert, resulted in decreased Mz-ChA-1 cell proliferation compared to controls (Figure 11A-C). Menin overexpression resulted in decreased cell migration and invasion by Boyden chamber and wound healing assays (Figure 11D-E).

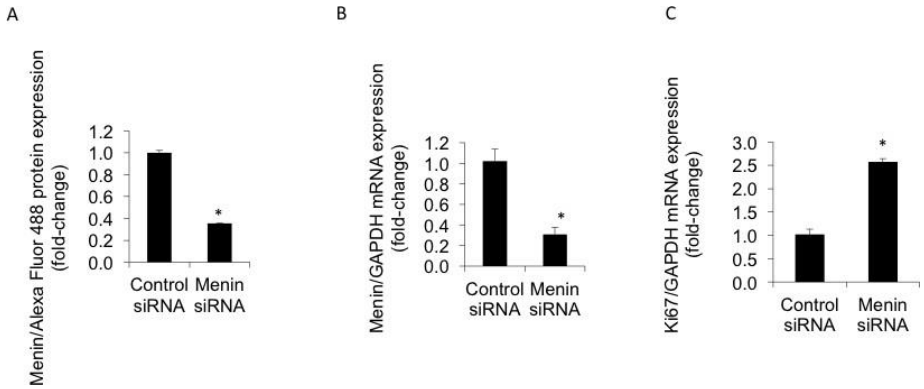

Figure 10: Downregulating menin increases CCA proliferation.
A-B: Menin siRNA decreases menin expression via flow cytometry and rtPCR, respectively. C. Decreased menin expression upregulates Ki67 proliferative marker *p 0.05 vs control.

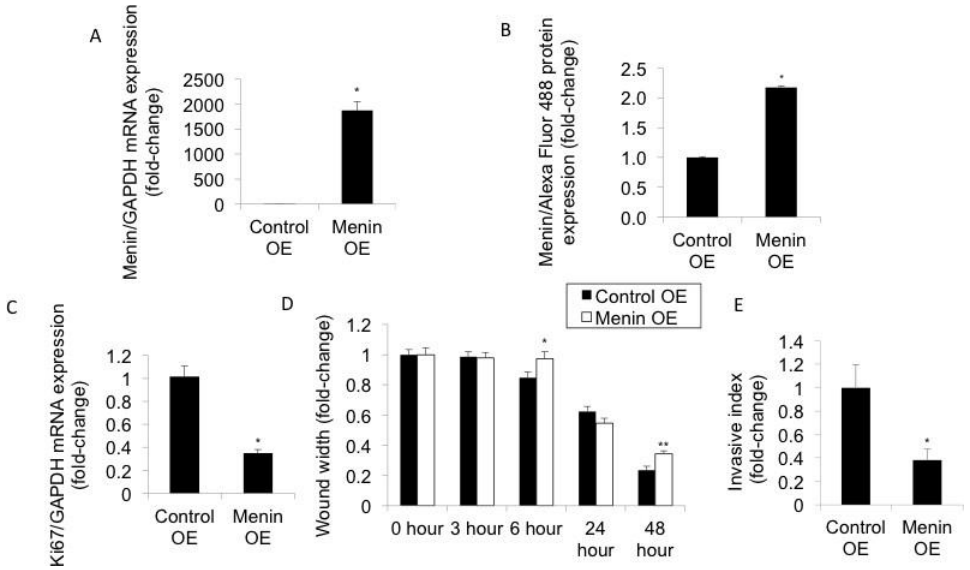

Figure 11: Overexpressing menin decreases CCA proliferation and cell migration.
A-B: Menin overexpression (OE) with pCMV6-MEN1 entry vector via rtPCR and flow cytometry, respectively. C. Menin overexpression decreases proliferation, wound healing, and cell invasion, respectively. *$p \leq 0.05$ vs control.

Effect of Changes on Menin Expression on Angiogenic and Proliferative Factors

Expression of the angiogenic factors VEGF-A/C, angiopoietins-1/2 (ANG-1/2), and the corresponding receptors VEGFR-2/3 (for VEGFs) and TIE1/2 (for angiopoietins- 1/2) were determined by real-time PCR following changes in MEN1 expression. The expression of the aforementioned increased in Mz-ChA-1 MEN1 KO (Figure 12A) cells and decreased in Mz-ChA-1 cells overexpressing menin (Figure 12B) compared to controls.

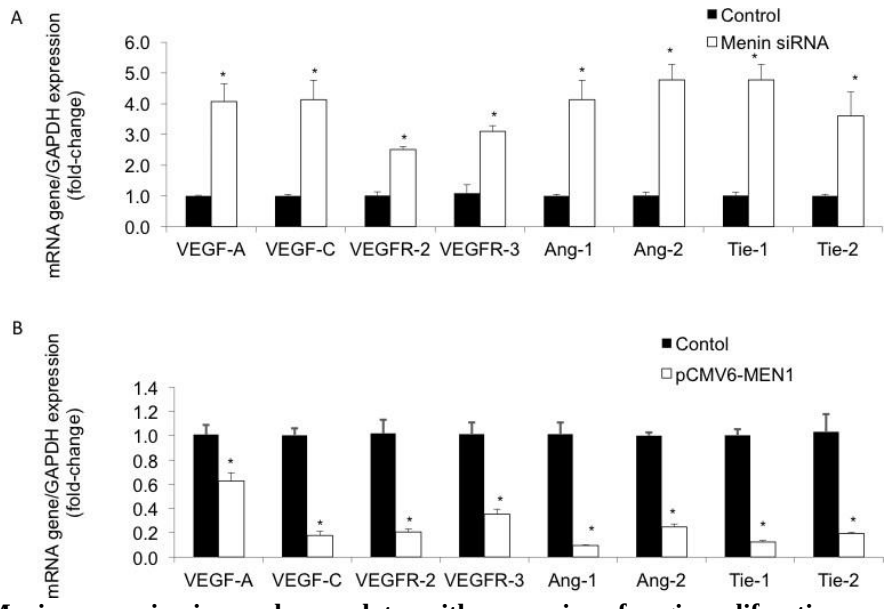

Figure 12: Menin expression inversely correlates with expression of angioproliferative markers in human CCA.

A-B: By rtPCR, expression of angiogenic factors inversely correlated to Men1 expression in Mz-ChA-1 CCA cell lines *$p \leq 0.05$ vs control.

Negative Regulation of Menin Expression by miR-24

We tested the hypothesis that miR-24 acts as a negative regulator of menin in cholangiocytes. We evaluated miR-24 expression in H69 and CCA cell lines by real-time PCR and demonstrated that miR-24 is overexpressed in the selected CCA lines compared to H69 cells (Figure 13A). We transfected pmirGLO-MEN1 vector into Mz-ChA-1 cells with a miR-24 mimic, hairpin inhibitor, or negative control and measured luminescence which demonstrated that miR-24 negatively regulates menin expression (Figure 13B). Finally, we obtained miRNA-seq data from 9 human CCA patients from the Cancer Genome Atlas Research Network (http://cancergenome.nih.gov/, last accessed April 7, 2016). We showed that miR-24 expression is increased compared to matched normal tissue (Figure 13C).

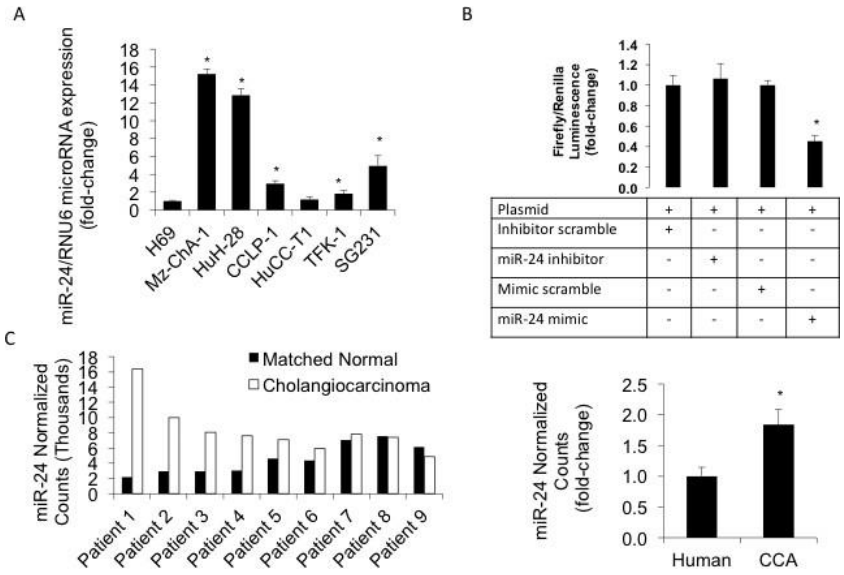

Figure 13: miR-24 is upregulated in human CCA.
A: miR-24 expression is increased in 5 of 6 human CCA cell lines. B: miR-24 mimic decreased MEN1 luminescence from luciferase construct. C: miRNA-sequence data from TCGA online database demonstrates increased miR-24 expression in 7 of 9 human CCA tumors compared to matched normal tissue. Statistical significance is validated with a Students unpaired t-test. *$p \leq 0.05$ vs control

We modulated miR-24 expression in Mz-ChA-1 cells and measured the expression of menin (FACS), angiogenic factors (by real-time PCR), cell proliferation (by MTS assays), cell migration by wound healing assay, and cell invasion by Boyden chamber assay. We knocked down miR-24 expression in Mz-ChA-1 cells using a hairpin inhibitor (Figure 14A). miR-24 downregulation correlated with increased menin expression (Figure 14B), decreased expression of angiogenic/proliferative factors (Figure 14C), decreased cell proliferation (Figure 15A), and decreased migration and invasion (Figure 15B-C).

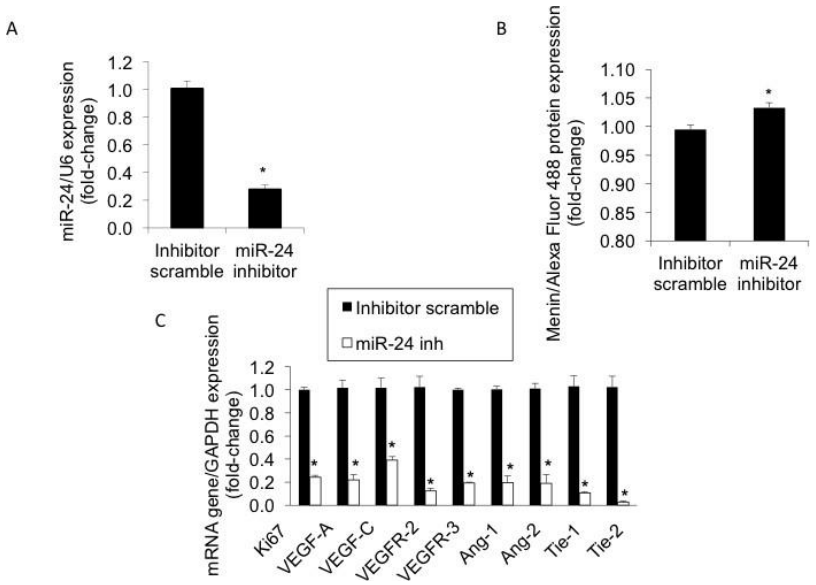

Figure 14: miR-24 increases menin expression and decreases angioproliferative marker expression.
A-B: miR-24 inhibition in Mz-ChA-1 cells decreases miR-24 expression and increases menin protein expression via flow cytometry, respectively. C: miR-24 inhibition decreases expression of angiogenic factors via rtPCR. *$p \leq 0.05$ vs control.

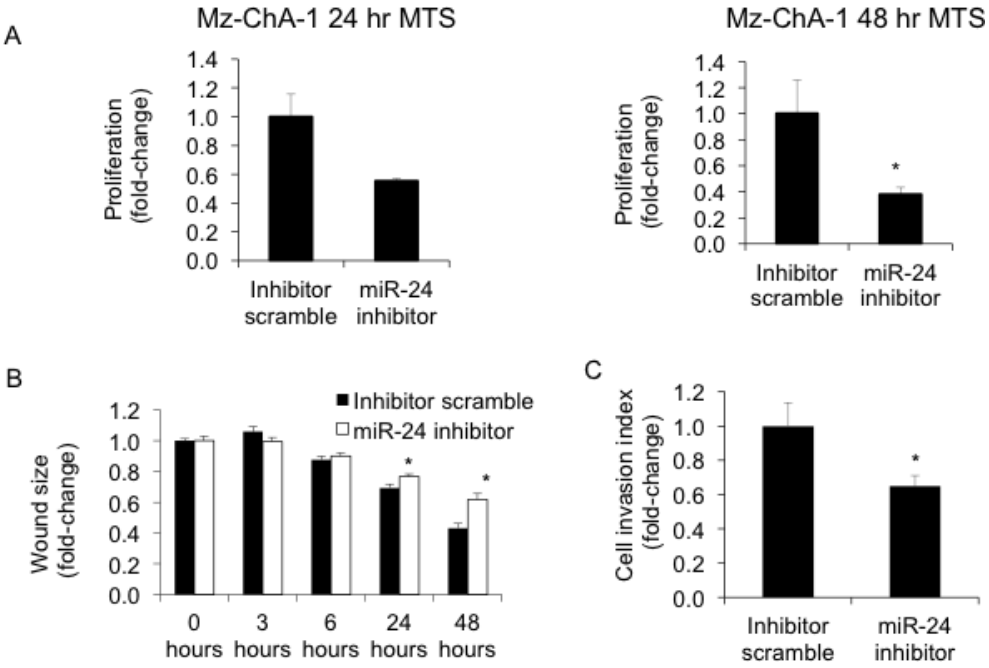

Figure 15: miR-24 inhibition decreases human CCA proliferation and migration.
A: miR-24 inhibition decreased proliferation in Mz-ChA-1 cells at both 24 hours left and 48 hours right time points. B-C: miR-24 inhibition decreased wound and cell invasion, respectively. *$p \leq 0.05$ vs control.

miR-24 Inhibitor Decreases Mz-ChA-1 Cell Growth in a Xenograft in Vivo Model

At the end of the treatment (10 weeks), as validation of our *in vivo* model, there was enhanced expression of menin in the tumor samples from the athymic mice treated with miR-24 hairpin inhibitor compared to scramble mismatch-treated mice (Figure 16B). Ten weeks following Mz-ChA-1 implantation into the flanks of nude mice, there was a significant reduction in tumor size in athymic mice treated with the miR-24 hairpin inhibitor compared to mice treated with mismatch scramble (Figure 16A). Real-time PCR performed on total RNA isolated from both tumor groups revealed decreased expression of proliferative and angiogenic factors (Figure 16C). Histological examination (Figure 17) demonstrated decreased proliferation via nuclear Ki67 staining, increased fibrosis via Sirius Red staining

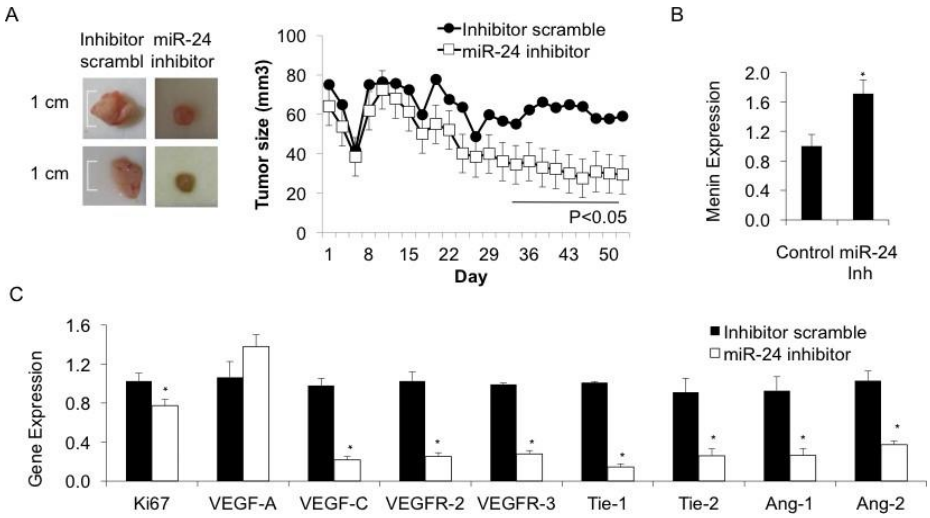

Figure 16: miR-24 inhibition decreases Mz-ChA-1 tumor burden.
A: 10 weeks following Mz-ChA-1 implantation into the flanks of nude mice, there was significant reduction in tumor size in athymic mice treated with the miR-24 hairpin inhibitor compared to scramble mismatch-treated mice. B. Inhibiting miR-24 expression in Mz-ChA-1 *ex vivo* tumors increases menin protein expression via flow cytometry. C: rtPCR on total RNA isolated from both tumor groups revealed decreased expression of proliferative and angiogenic factors. (n=3). *p 0.05 vs control.

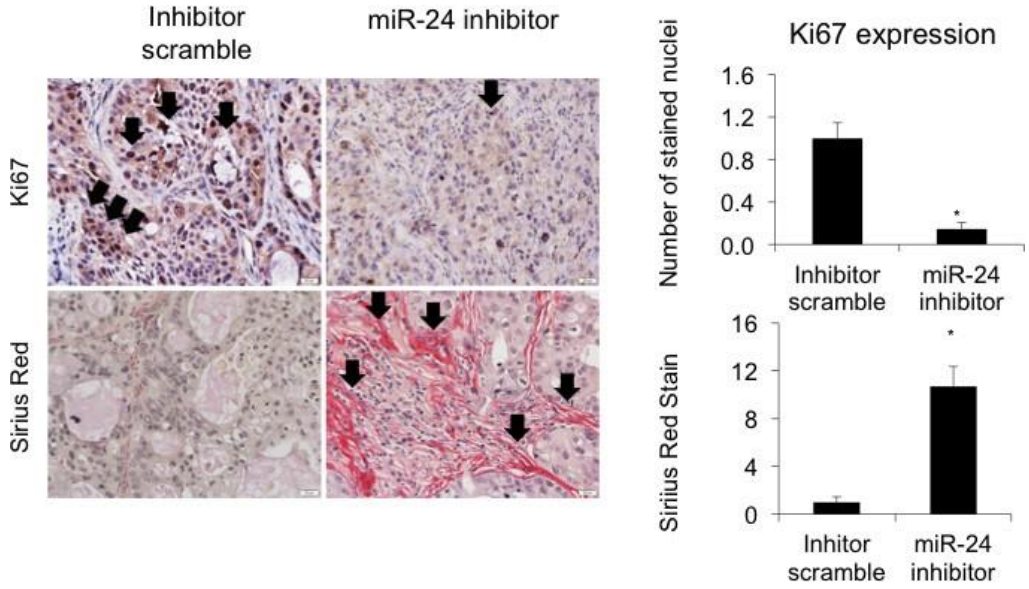

Figure 17: miR-24 inhibition decreases proliferation but increases fibrosis in Mz-ChA tumors.
IHC images of FFPE sections confirm expected histological depictions of Mz-ChA-1 CCA tumor via H&E and CK-19 staining (not shown). Top Row miR-24 inhibition decreased nuclear Ki67 staining (quantification on right). Bottom Row miR-24 inhibition increased collagen deposition and fibrosis via Sirius Red staining (n=3). * $p \leq 0.05$ vs control.

3.5 Discussion

This novel study demonstrated that menin acts as a tumor suppressor in malignant cholangiocytes and is downregulated in human CCA. Overexpressing menin *in vitro* decreases migration, invasiveness, proliferation and angiogenesis, whereas knocking down menin expression *in vitro* increases proliferation and angiogenesis. Furthermore, we show that miR-24 acts as an oncogene partly through its negative regulation of menin expression via binding to its 3' UTR. Knocking down miR-24 expression with a hairpin inhibitor increases menin expression and decreases proliferation, migration, invasiveness, and angiogenesis both *in vitro* and *in vivo* xenograft models.

In addition to menin's canonical role in the MEN1 familial cancer syndrome, it is associated with a host of other cancers and proliferative pathologies. For example, loss of menin drives G cell proliferation in the stomach leading to hyperplasia and hypergastrinemia (28). Menin suppresses proliferation and migration in lung carcinoid tumors, non-small cell lung cancer, and lung adenocarcinoma (27). Yan et al. revealed that menin interacts with scaffold protein IQGAP1 in the β-cell cytoplasm to decrease cell motility and increase cell adhesion through enhanced E-cadherin and β-catenin intercellular junctions (119). Koen et al. reported mutations in the MEN1 gene disrupted menin's co-activation of estrogen receptor-mediated transcription in breast cancer cells (99). However, menin is not necessarily tumor suppressive in all tissues. Menin overexpression is correlated with growth of prostate tumors (100). Functional menin expression is required for leukemogenesis in MLL in order to drive transcription of mutant

MLL-fusion protein targets (120).

Menin's role in HCC formation is controversial. One study showed that menin interacts with Sirt1, a type III histone deacetylase (HDAC), to inhibit NF-κB-mediated transactivation of inflammatory cytokines in HCC (29). A contradicting study showed that the menin-MLL interaction epigenetically enhances Yap1 transcription factor expression to drive HCC formation (66). However, no information has previously been published regarding the role of menin in CCA formation and progression.

Menin mainly acts in concert with scaffold proteins to drive histone methylation or deacetylation depending on its binding partners and its tissue of origin; however, other histone marks have been associated with menin activity. In G cells, menin binds to and inhibits JunD transcriptional activation by recruiting HDACs to JunD target sites and removing transcriptionally activating histone acetylation marks (28). In pancreatic β-cells, the menin-MLL complex enables transcriptionally activating H3K4 trimethylating marks at MLL target genes. In particular, this drives expression of the CDKi proteins p27Kip1 and p18INK4c to suppress proliferation (121).

In this study, we show that menin expression negatively regulates angiogenic and proliferation markers in cholangiocytes. Cholangiocytes secrete and respond to VEGF in an autocrine and paracrine manner to promote proliferation (122). No evidence to date points to a role for menin in angiogenesis. However, histone acetylation dynamics are closely connected with epigenetic regulation of angiogenesis (123). In particular, JunD plays a major role in combating hepatic ischemic/reperfusion injury through

antagonizing other AP-1 transcription factors to regulate HIF-1α and VEGF-A expression (124).

In this study, we decreased miR-24 expression with a hairpin inhibitor to increase menin protein expression and inhibit proliferation, angiogenesis, migration, and invasion in human Mz-ChA-1 cell lines, using both *in vitro* and *in vivo* xenograft models. miR-24 is upregulated in a host of gastrointestinal cancers, and pancreatic cancer xenograft models overexpressing lentiviral miR-24 grew larger tumors compared to controls (101-104). However, miR-24 has not yet been characterized in biliary disease. miR-24 is implicated in many cellular processes including cell cycle, apoptosis, DNA repair (47), proliferation, migration, and angiogenesis (44).

Melatonin negatively regulates miR-24 expression in several cancers to inhibit tumor proliferation and migration, and lower melatonin signaling in cholangiocytes leads to increased VEGF expression (47). MiR-24 expression is increased HCC and its inhibition reduces proliferation, migration, and invasion (48).

Menin expression can be modulated by other factors as well. Prolactin and glucose stimulation decrease menin expression and increases proliferation in β-cells whereas insulin signaling decreases menin expression (23). TGF-β1 and somatostatin signaling increase menin expression in hepatocytes and the duodenum, respectively (25). Small molecule inhibitors can block pathway-specific menin functions without altering its overall expression levels. For example, HDAC inhibitor class 1/2 trichlorostatin A

reverses menin-dependent transcriptional repression at JunD target sites (25, 125). The menin-MLL inhibitor can block menin-dependent MLL histone trimethylation.

In summary oncogene miR-24 and tumor suppressor menin work together in a negative feedback loop to maintain cholangiocyte homeostasis. Dysregulation of this network alters expression of cell cycle and apoptotic genes leading to increased proliferation, migration, and angiogenesis. Targeting miR-24 expression represents a novel means to increase menin expression and reduce biliary tumor growth. Other means of targeting menin expression and/or function include hormonal therapy or small molecule inhibitors such as menin-MLL or HDAC inhibitors.

4 α7-NACHR KNOCKOUT MICE DECREASES BILLIARY HYPERPLASIA AND LIVER FIBROSIS IN CHOLESTATIC BILEDUCT LIGATED MICE [4]

4.1 Overview

α7-nAChR is a nicotinic acetylcholine receptor specifically expressed on hepatic stellate cells, Kupffer cells, and cholangiocytes that regulates inflammation and apoptosis through intracellular [Ca2+] increase and activation of ERK1/2. Thus, targeting α7-nAChR may be therapeutic in biliary disease. Bile-duct ligation (BDL) was performed on wild-type (WT) and α7-nAChR$^{-/-}$ mice, with sham-operated mice as controls. Gene expression of α7-nAChR, Ki67/PCNA (proliferation), and TGF-β1, fibronectin-1, Col1α1, and α-SMA (fibrosis) was measured with real-time PCR. Immunohistochemistry (IHC) was performed to assess bile-duct mass (Ck-19), and Sirius Red staining was performed to quantify the amount of collagen deposition. Immunofluorescence was performed to assess co-localization of α7-nAChR with bile duct (Ck-19) and hepatic stellate cells (desmin). Biliary TGF-β1 expression was assessed using IHC, and serum chemistry measured to assess liver damage. Stable α7-nAChR$^{-/-}$ pooled cholangiocytes were subject to mechanical stress similar to biliary pressure following BDL, and menin expression was measured. α7-nAChR$^{-/-}$ mice

[4] § Part of this chapter is reprinted with permission from L. Ehrlich, A. O'Brien, C. Hall, T. White, L. Chen, N. Wu, J. Venter, M. Scrushy, M. Mubarak, F. Meng et al. α7-nAChR Knockout Mice Decreases Biliary Hyperplasia and Liver Fibrosis in Cholestatic Bile-Duct Ligated Mice. Gene expression, 2018.

exhibited decreased bile duct mass and fibrosis following BDL compared with WT mice. Expression of fibrotic marker genes and biliary TGF-β1 was also decreased. α7-nAChR co-localizes with Ck-19 and desmin and α7-nAChR$^{-/-}$ BDL show reduced Ck-19 and desmin expression compared to WT BDL. Furthermore, menin expression increases following mechanical stress but is reduced in α7- nAChR$^{-/-}$ cells. α7-nAChR activation drives biliary proliferation and fibrosis in BDL model, possibly through induction of menin expression, and may be a therapeutic target in combating extra-hepatic biliary obstruction.

4.2 Introduction

Cholangiocytes are epithelial cells that line the bile duct system and are the main targets of cholangiopathies (126, 37). Cholangiopathies, while broad in etiology, are characterized by cholestasis, ductular reaction, and liver damage (127). Extra-hepatic bile duct obstruction, mimicked by bile-duct ligation (BDL) in mice, increases pressure across the biliary tree leading to increased intrahepatic bile duct mass (IBDM) and bridging fibrosis between intra-hepatic portal triads (2, 128). In contrast, primary sclerosing cholangitis (PSC), a well-known autoimmune cholangiopathy, results in irregular bile duct proliferation, periductal fibrosis, and bridging necrosis which progresses to cirrhosis and the need for liver transplantation (129, 130).

Vagal stimulation of the hepatic cholinergic system is anti-inflammatory and anti-apoptotic and is strongly mediated by α7-nAChR activation (131, 132). It is important to recognize distinct dynamics between nicotine and acetylcholine (endogenous physiological stimulants of nAChRs). While extracellular acetylcholine is quickly degraded by acetylcholinesterase (small fraction of a second), nicotine has a much longer half-life (2 hours) and therefore stimulates nAChR for a longer time period before being degraded and cleared (133). Acetylcholine also acts through muscarinic AChRs, which nicotine does not, to drive cholangiocyte proliferation and secretin-dependent choleresis in a cAMP-dependent fashion following BDL (134) as well as hepatic stellate cell activation and fibrogenesis in an PI3K- and MEK-dependent pathway (135).

There remains considerable controversy on the effects of smoking and the pathogenesis of certain biliary diseases, particularly PSC (136). In particular, there is small but significant epidemiological data indicating that smoking may be protective in PSC patients who are male or who have concomitant ulcerative colitis (UC) (136, 137). Patients with PSC are less likely to smoke and male daily smokers experienced later onset of disease compared to non-smoking male counterparts (136). While smoking may increase the incidence of CCA in patients with PSC, it may be protective in the subtype of PSC with concomitant inflammatory bowel disease (IBD) (138, 139). Of course, smoking increases the incidence of colorectal cancer in patients with IBD, which is in itself a risk factor for CCA onset.

With regards to extra-hepatic causes of cholestasis, smoking is not associated with onset of gallstones, however smoking is an independent risk factor for the onset of gallbladder cancer in patients with underlying gallstones (140). We have previously shown that rats treated with nicotine by osmotic minipump exhibited increased cholangiocyte proliferation, which is consistent with its pro-cholinergic, anti-inflammatory, and anti-apoptotic effects (141). Nicotine treatment also increased expression of fibrotic genes and α7-nicotinic receptor (141). We have also shown that nicotine increases growth and proliferation of CCA xenograft tumors, which is abrogated in α7-nAChR$^{-/-}$CCA tumors (142). In this paper, we sought to characterize the role of α7-nAChR in BDL mice, a model of extra-hepatic cholestasis characterized by increased biliary proliferation and fibrosis.

There is little literature regarding the relationship between the miR-24/menin axis and

nAChR signaling. Emerging evidence points to a role for menin in determining nAChR subunit expression and surface clustering in hippocampal neurons. In central neurons from invertebrates, the full length menin protein and its N-terminal proteolytic fragment localize to the nucleus whereas the C-terminal proteolytic fragment localizes at synapses. The C-terminal fragment coordinates $\alpha 7$-nAChR subunit clustering which is abrogated following knockdown of MEN1 expression (143, 144). However, little is understood about menin proteolytic fragments or regulation of $\alpha 7$-nAChR subunit surface clustering in liver physiology.

4.3 Materials and Methods

Materials

Reagents were purchased from Sigma Aldrich (St. Louis, MO), unless otherwise indicated. α7-nAChR shRNA was purchased from Qiagen (KH22901, Valencia, CA) and transfected with Lipofectamine®2000 Transfection reagent (ThermoFisher Scientific, Grand Island, NY). The following antibodies were purchased from Abcam (Cambridge, MA): a7-nAChR (ab24644); cytokeratin-19 (CK-19, ab52625). α7-nAChR (Chrna7, NM 007390); CK-19 (Krt19, PPM02968A); Ki67 (Mki67, PPM03457B); PCNA (PPM03456F); Collagen Type I Alpha 1 (Col1α1, PPM03845F); fibronectin-1 (Fn-1, PPM03786A); α-smooth muscle actin-2 (α-SMA, PPM04483A); Transforming Growth Factor β1 (TGF-β1, PPM03845F); and fibronectin-1 (Fn-1, PPM03786A);

Animal Models

Animal protocols were approved by the Baylor Scott & White Institutional Animal Care and Use committee. Male C57BL/6 (wild-type, WT, 12-week age, 25-30 gm) and α7-nAChR$^{-/-}$ mice (12-week age, 25-30 gm) were purchased from Jackson Laboratory (Bar Harbor, ME), housed in a temperature-controlled environment (22 ^{o}C) with 12:12-hr light-dark cycles, and fed standard rodent chow with access to water ad libitum. Briefly, the last exons of the Chrna7 gene were deleted and a KO mouse was generated on a mixed 129/SvEv and C57BL/6 background and eventually bred to a C57BL/6 background. Both WT and α7-nAChR$^{-/-}$ mice were subject to either sham or BDL surgery (14) and utilized 3 or 7 days later.

Cell Isolation

Following sham or BDL, total liver samples were harvested from the mice and used for the preparation of frozen or paraffin-embedded liver sections by standard techniques. Serum was also collected. Cholangiocytes were isolated by standard immunoaffinity separation (3) (145) by using a monoclonal antibody, rat IgG2a (a gift from Dr. R. Faris, Brown University, Providence, RI) that recognizes an unidentified antigen expressed by all intrahepatic cholangiocytes.

Immunoreactivity for α7-nAChR and TGF-β and TGF-β Activity for Unidentified Antigen Expressed by all Intrahepatic Cholangiocytes

IHC for α7-nAChR and TGF-β was performed on paraffin-embedded liver sections (4-5 μm) from the selected groups of mice as described (146). Biliary TGF-β immunoreactivity was measured in intrahepatic bile ducts as the staining intensity per bile duct field using the Olympus Image Pro-Analyzer software (Olympus, Tokyo, Japan); values were normalized to normal WT liver sections. We also evaluated by immunofluorescence in frozen liver sections (4-5 μm thick) the expression of α7-nAChR in bile ducts (co-stained with CK-19, a cholangiocyte-specific marker) (145) as well as hepatic stellate cells (HSCs, co-stained with desmin, a marker of HSCs) (147). Immunofluorescent sections were mounted with DAPI (Invitrogen), to stain for cell nuclei, and imaged with a confocal microscope (Olympus FluoView 500 laser scanning microscope with DP70 digital camera, Tokyo, Japan). CK-19 values were normalized to normal WT sections; α7-nAChR basal expression in normal WT slides were too low to normalize so values were therefore

expressed as relative changes.

We measured liver fibrosis by: (i) Sirius Red staining in liver sections (4-5 μm thick, 10 fields analyzed from 3 different samples from 3 different animals); and (ii) measurement of hydroxyproline levels in total liver samples using the Hydroxyproline Assay Kit (MAK008; Sigma-Aldrich). Following Sirius Red staining, slides were scanned by a digital scanner (Leica Microsystems, SCN400, Buffalo Grove, IL) and staining quantified using Image-Pro Premier 9.1 (Media Cybernetics, MD).

Real-time PCR in Total Liver Samples

Total RNA was isolated from snap-frozen samples from total liver and purified cholangiocytes using the Ambion mirVana™ isolation kit (Ambion, Austin, TX) as described (146). cDNA was created with 5x iScript™ Supermix (BIO-RAD, Hercules, CA) according to the vendor's protocol. Real-time PCR analysis of the selected samples were performed using 1 μg of total RNA with the SYBR Green real-time PCR kit (SABiosciences, Frederick, MD) with glyceraldehyde-3-phosphate dehydrogenase (GAPDH) as the housekeeping gene (148).

Cell Lines

In vitro studies were performed on our immortalized intrahepatic murine cholangiocyte lines (ICMLs) (148) (149). α7-nAChR expression was knocked down using α7-nAChR shRNA (KH22901) with Lipofectamine® 2000 Transfection reagent (ThermoFisher Scientific, Grand Island, NY) according to vendor's protocol. Knockdown of α7-nAChR

expression was confirmed by real-time PCR (148). MTS assays were used to assess cell proliferation using CellTiter 96™ Aqueous One Solution according to the vendor's instructions (Promega, Madison, WI) (14).

In Vitro Models Mimicking BDL in WT and α7-nAChR-/- Cholangiocytes

Cells were plated on Flexcell® 6-well membrane plates (Flexcell®, Burlington, NC) and subjected to biaxial mechanical stress on a Flexcell® FXSK™ Tension system for 12 hours (Flexcell®, Burlington, NC). Controls were plated on the same plates but not subjected to mechanical stress. The cells were harvested and RNA was isolated according to the aforementioned protocols. MEN1 gene expression was measured.

4.4 Results

Mechanical Stress Decreased Menin Expression in α7-nAChR Knockout Cholangiocytes Compared to WT Cholangiocytes

Following 12 hours of mechanically-induced stress, menin expression increased in WT and control cells while decreasing in α7-nAChR$^{-/-}$ICMLs (Figure 18).

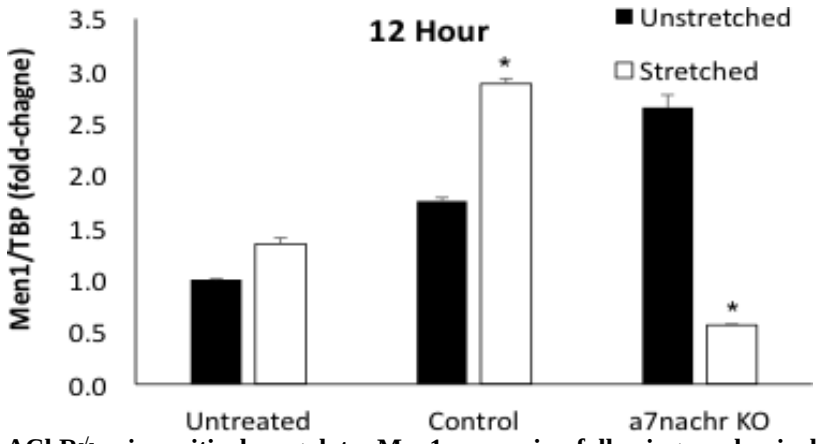

Figure 18: α7-nAChR$^{-/-}$ axis positively regulates Men1 expression following mechanical stress. ICMLs subject to 12 hours of mechanical stretch increased Men1 gene expression. However, ICMLs lacking the α7-nAChR had a decrease in Men1 gene expression. *$p \leq 0.05$ vs matched unstretched group.

Expression of α7-nAChR

There was increased immunoreactivity for α7-nAChR in liver sections from BDL WT compared to WT mice; immunoreactivity for α7-nAChR was absent in both normal and BDL α7-nAChR$^{-/-}$mice (Figure 19A-C). The localization of α7-nAChR in intrahepatic bile ducts (red color co-stained in green with CK-19) and in HSCs (green color in HSCs co-stained in red with desmin) was also confirmed by immunofluorescence (Figure 19C).

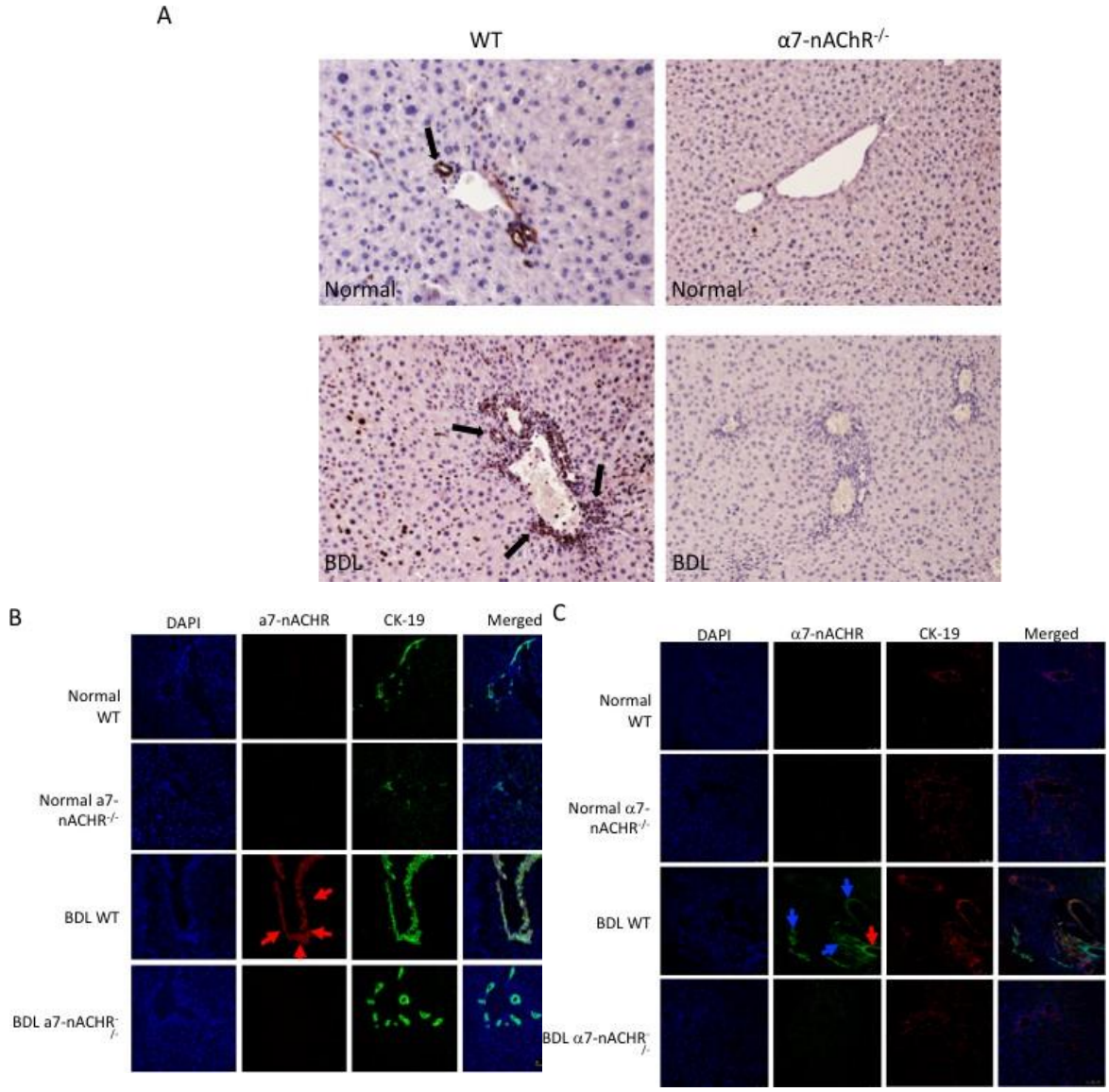

Figure 19: Loss of *α*7-nAChR expression in *α*7-nAChR$^{-/-}$ mouse model.
[A-C] There was increased immunoreactivity for *α*7-nAChR in liver sections from BDL WT compared to WT mice; immunoreactivity for *α*7-nAChR was virtually absent in both normal and BDL *α*7-nAChR$^{-/-}$ mice. Orig. magn., x25. [B-C] By immunofluorescence, we demonstrated the immunoreactivity of *α*7-nAChR in bile ducts (red color co-stained in green with CK-19) and in HSCs (green color in HSCs co-stained in red with desmin) was also confirmed by immunofluorescence. Nuclei are stained in blue with DAPI.

α7-nAChR-/- Mice Exhibit Lower Biliary Proliferation Following BDL

There was increased IBDM in BDL mice compared to WT mice. However, there was a significant decrease in IBDM in α7-nAChR$^{-/-}$ BDL mice compared to WTBDL (Figure 20A-B). BDL-induced increase in Ki67A gene expression was reduced in α7-nAChR$^{-/-}$BDL compared to WT BDL mice (Figure 20C).

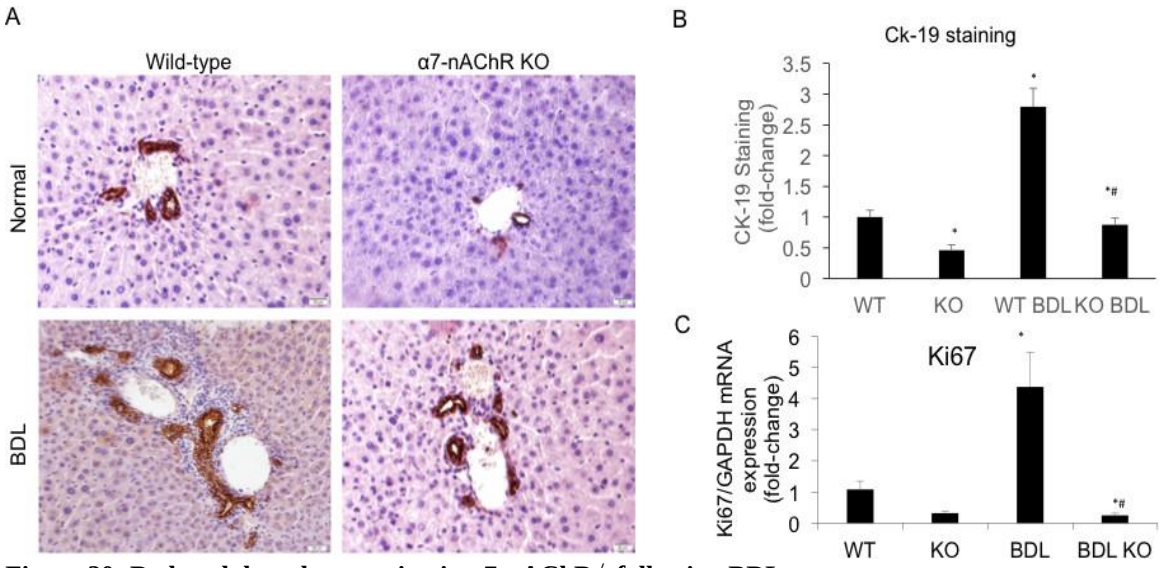

Figure 20: Reduced ductular reaction in α7-nAChR$^{-/-}$ following BDL.
A-B: Immunohistochemical analysis shows increased IBDM in BDL WT mice com- pared to normal WT, but decreased IBDM in BDL α7-nAChR$^{-/-}$ compared to WT BDL mice. Ki67 expression is decreased in BDL α7-nAChR$^{-/-}$ compared with WT BDL. *P < 0.05 vs. normal WT mice. #P < 0.05 vs. BDL WT mice.

Biliary Fibrosis is Decreased in α7-nAChR-/- Mice Following BDL

Sirius Red staining for collagen deposition and hydroxyproline levels both increased in WT BDL compared to normal WT mice but decreased in α7-nAChR$^{-/-}$ BDL mice compared to WT BDL (Figure 21A-C). Additionally, gene expression of the fibrosis markers α-SMA, TGF-β1, Col1α1, and Fn-1 decreased in total liver samples from α7-nAChR$^{-/-}$ BDL mice compared to WT BDL mice (Figure 21).

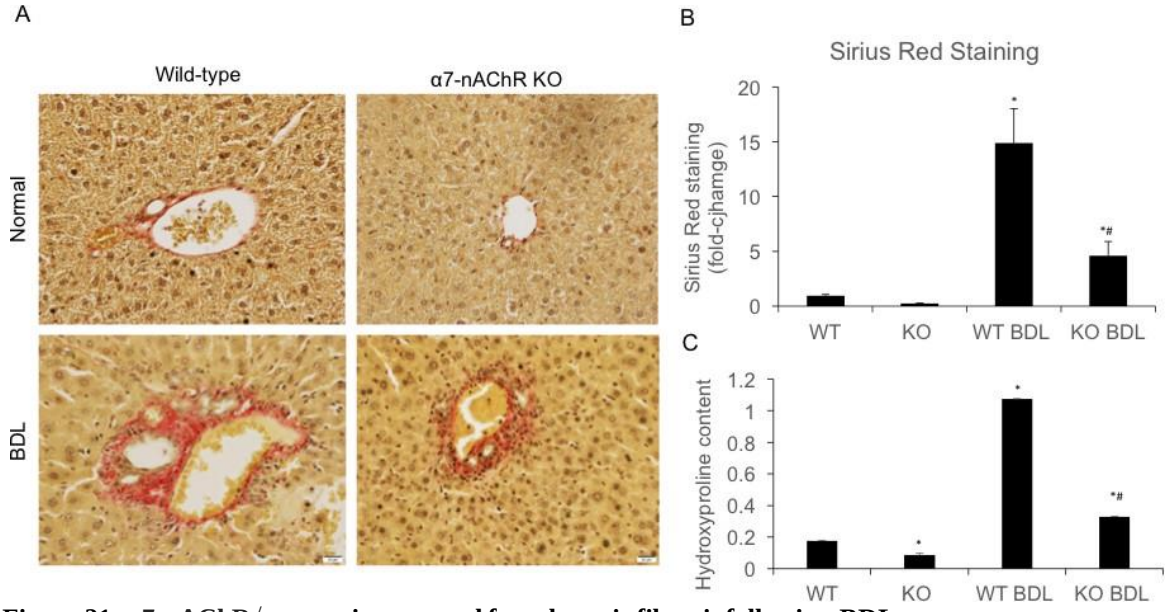

Figure 21: α7-nAChR$^{-/-}$ mouse is protected from hepatic fibrosis following BDL.
A-B: Sirius Red staining reveals increased fibrosis in BDL W mice compared to normal WT, but decreased collagen deposition in α7-nAChR$^{-/-}$ BDL mice compared to WT BDL C: Hydroxyproline assay reveals decreased hydroxyproline content in α7-nAChR$^{-/-}$ BDL mice compared to WT BDL. (n=3). *P <0.05 vs. normal WT mice. #P < 0.05 vs. BDL WT mice.

As shown in Figure 22, the biliary immunoreactivity of TGF-β1 greatly increased in liver sections from BDL WT mice (compared to normal WT mice) but was attenuated in α7-nAChR$^{-/-}$BDL mice; no significant difference in TGF-β1 immunoreactivity was observed between normal WT and α7-nAChR$^{-/-}$mice.

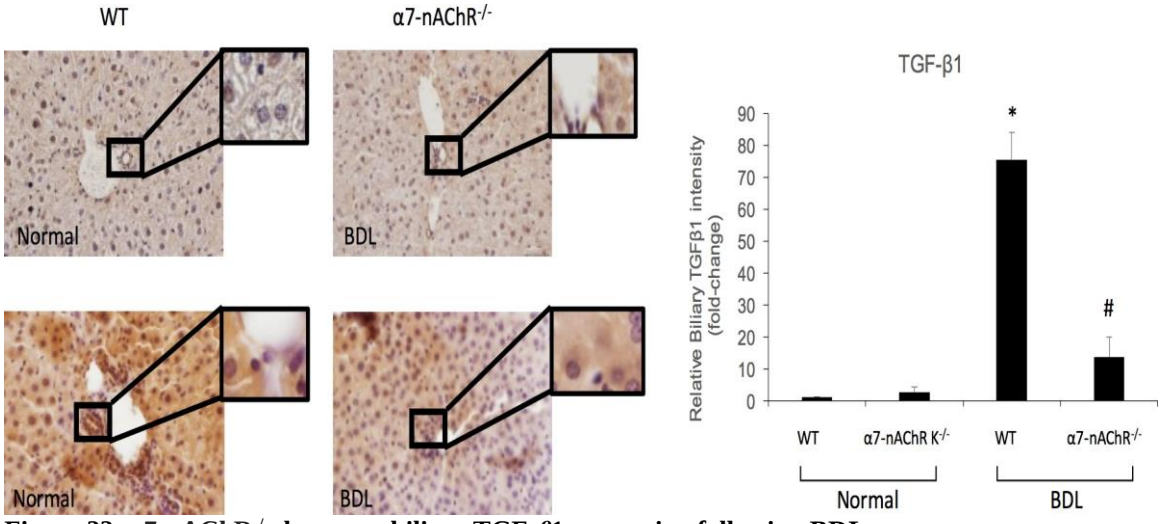

Figure 22: α7-nAChR$^{-/-}$ decreases biliary TGF-β1 expression following BDL.
Immunohistochemical analysis reveals increased biliary TGF- β1 immunoreactivity BDL mice compared to WT mice, but reduced immunoreactivity in α7- nAChR-/- BDL mice compared to WT BDL (n=3). *P < 0.05 vs. normal WT mice. #P < 0.05 vs. BDL WT mice.

Kupffer Cell Infiltration and Expression of Inflammatory Markers are Reduced in α7-nAChR$^{-/-}$ Mice Following BDL

CD68 immunoreactivity was used to assess Kupffer cell infiltrate from the selected groups of mice. Kupffer cell infiltration increased following BDL but decreased in BDL α7-nAChR$^{-/-}$ mice (Figure 23). By real-time PCR, the expression of IL-6, IL-1β, and TNFα increased in cholangiocytes from BDL mice (compared to WT mice) but decreased in BDL α7-nAChR$^{-/-}$ mice compared to BDL WT mice (Figure 24).

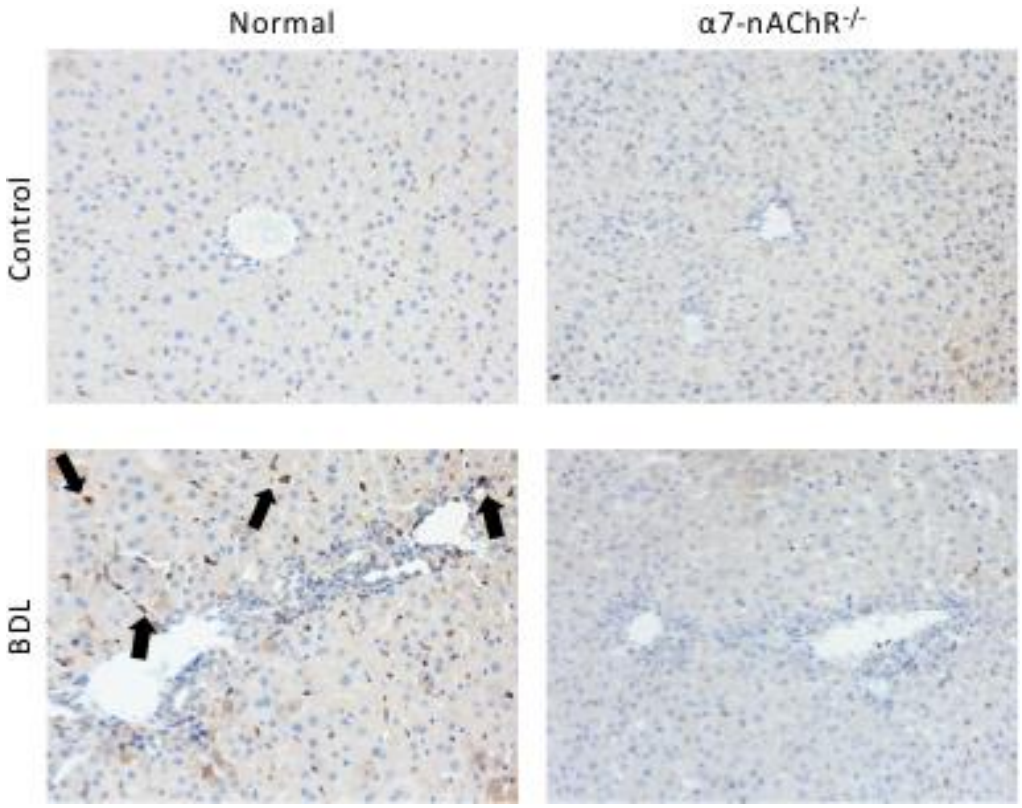

Figure 23: CD68 immunoreactivity is decreased in *α*7-nAChR$^{-/-}$ BDL compared to BDL WT mice. CD68 immunoreactivity was used to assess Kupffer cell infiltration in selected mice groups. Figure 6 shows that Kupffer cell infiltration increases following BDL but decreases in *α*7-nAChR$^{-/-}$ BDL mice. Black arrows are used to point out the CD68^{+} Kupffer cells. Orig. magn., x20.

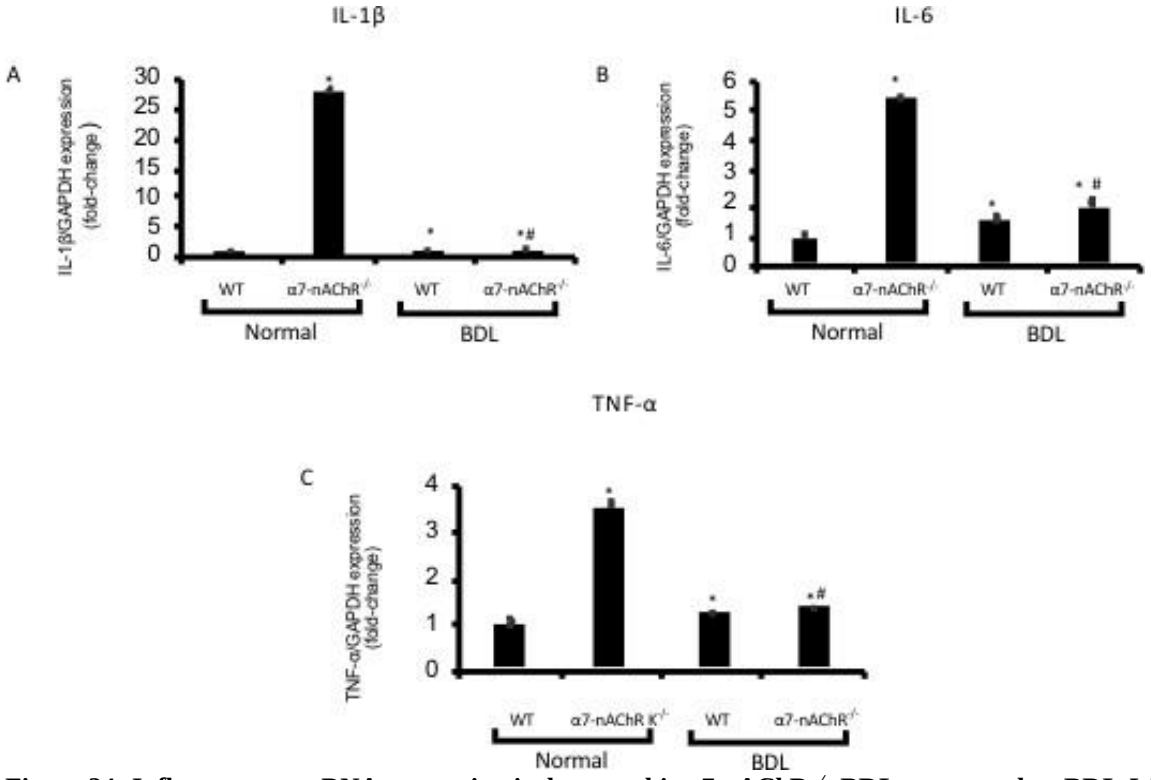

Figure 24: Inflammatory mRNA expression is decreased in α7-nAChR$^{-/-}$ BDL compared to BDL WT mice.

[A-C] Gene expression for IL-1β, IL-6, and TNFα increased in cholangiocytes from WT BDL compared to normal WT mice, but decreased in α7-nAChR$^{-/-}$ BDL compared to WT BDL mice. Data are mean±SEM performed in triplicate in 3 different total liver samples from 3 mice. *P $\leq$ 0.05 vs. normal WT mice. #P $\leq$ 0.05 vs. BDL WT mice.

Expression of Bile Acid Synthesis and Transport Genes Reduced in α7-nAChR$^{-/-}$ Mice Following BDL

The mRNA expression of CYP7A1, CYP27A1, and BSEP (proteins playing important roles in bile acid metabolism) (150) increased following BDL and decreased in BDL α7-nAChR$^{-/-}$ mice (Figure 25).

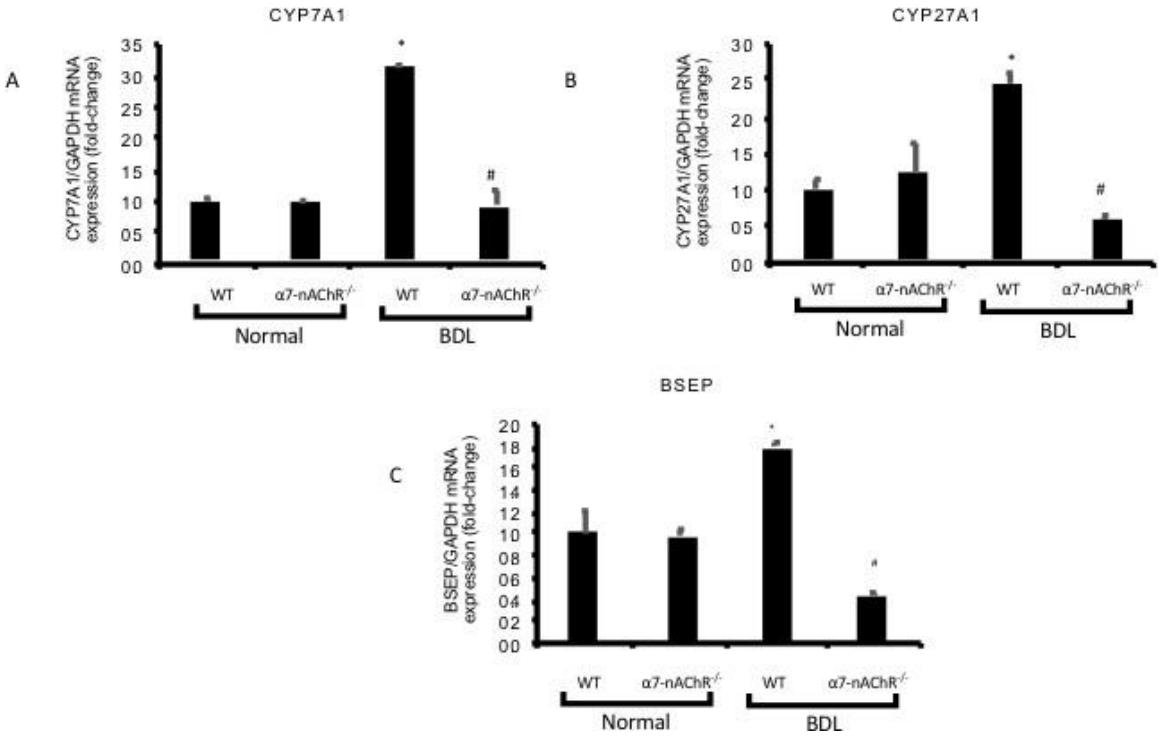

Figure 25: Expression of bile acid synthesis and transport genes reduced in α7-nAChR$^{-/-}$ mice following BDL.
[A-C] Gene expression ofCYP7A1, CYP27A1, and BSEP increased following BDL and decreased in BDL α7-nAChR$^{-/-}$ mice. Data are mean±SEM performed in triplicate in 3 different total liver samples from 3 mice. *P $\leq$ 0.05 vs. normal WT mice. #P $\leq$ 0.05 vs. BDL WT mice.

4.5 Discussion

We have previously shown that chronic nicotine exposure stimulates biliary growth and hepatic fibrosis (141) (142). In this study, we used total body knockouts of α7-nAChR to explore its specific effects on a BDL mouse model of cholestatic injury. Mice lacking the α7-nAChR who underwent BDL exhibited less biliary proliferation and hepatic fibrosis compared to their WT counterparts, (brought about by receptor-mediated interaction with both cholangiocytes and HSCs) compared to their WT counterparts. We also observed increased immunoreactivity of TGF-β1 in liver sections from BDL mice compared to normal WT mice, immunoreactivity that decreased in α7-nAChR BDL mice compared to BDL WT mice. Furthermore, we confirmed that α7-nAChR co-localized with both bile ducts (Ck-19) and HSCs (desmin), and that α7-nAChR$^{-/-}$ BDL mice expressed less activated HSCs compared to WT counterparts. On the basis of these findings, we propose that the decrease in biliary proliferation/ductal mass and liver fibrosis is mediated by decreased expression of α7-nAChR in cholangiocytes and HSCs, respectively. Since we have previously shown that the activation of HSCs and increased liver fibrosis is mediated by enhanced biliary TGF-β1 expression/secretion (148), we also proposed a paracrine mechanism by which a decrease in biliary TGF-β1 immunoreactivity/expression (mediated by knock-out of α7-nAChR) contribute to reduced liver fibrosis.

α7-nAChR and menin appear to play similar pro-fibrotic roles in the BDL mouse model. Both are upregulated following expression, and inhibiting both rescues the fibrotic

phenotype. Furthermore, we demonstrate that increased menin expression following mechanical stress is abrogated by knocking out α7-nAChR expression *in vitro*. As described above, menin can mediate TGF-β1 signaling through interaction with nuclear p-SMAD proteins and initiate transcription of target genes. Thus, it would appear that the α7-nAChR axis might interact with menin through the TGF-β1 signaling pathway.

α7-nAChR is part of the vagal cholinergic system that responds to acetylcholine released by postganglionic efferent nerves (151), although both nicotinic and muscarinic receptors can bind to acetylcholine. α7-nAChR expression has been measured in in HSCs (152), Kupffer cells (132) as well as cholangiocytes (141). Various mouse models of liver damage have been used to study the effects of vagal stimulation and/or α7-nAChR activation but have resulted in somewhat differing conclusions. For example, it is well established that vagal nerve firing releases acetylcholine that binds to α7-nAChR on Kupffer cells and reduces their activation and subsequent hepatic inflammation (132, 153). However, acetylcholine can also bind to muscarinic receptors directly on HSCs and promote a pro-fibrogenic phenotype (135). We have previously shown nicotine acts on cholangiocytes in a α7-nAChR-specific manner to increase biliary proliferation and fibrosis (141, 142).

Cigarette smoke is strongly associated with colon and pancreatic cancer yet epidemiological evidence for its role in liver diseases is less clear, particularly due to confounding factors such as alcohol intake (154). While it is generally agreed that smoking contributes to liver disease, particularly hepatocellular carcinoma and cholangiocarcinoma (CCA), it is believed to exacerbate liver injury in partnership with other genetic and environmental

insults. For example, smoking is strongly associated with tumorigenesis in patients with chronic hepatitis C, PSC, primary biliary cholangitis (PBC), and gallstones (140) (154). Cigarette smoke contains over 4,000 chemicals among which nicotine provides the psychoactive and addictive properties. There is a host of literature implicating α7-nAChR in the liver-tropic effects of nicotine (131, 132, 141, 152, 155). Nicotinic acetylcholine receptors (nAChR) are ionotropic, as opposed to G-protein coupled muscarinic acetylcholine receptors, which are metabotropic, and are formed from homo- or hetero- pentameric assembly of nAChR subunits α1-10, β1-4, γ, δ, and E (156). All forms are present in the central nervous system, however, liver expression of α7-nAChR is limited to hepatic stellate cells (152), Kupffer cells (132) and cholangiocytes (141).

Activated cholangiocytes take on a neuroendocrine-like phenotype that secretes and responds to neuropeptides and hormones in an autocrine and paracrine fashion (157). In the BDL mouse model, extrahepatic bile duct blockage increases pressure along the biliary tree and causes a toxic buildup of bile acids that leads to biliary damage, ductular reaction, and hepatic fibrosis (158). It is thought that HSCs, or even portal fibroblasts, contribute to the fibrotic reaction through cross-talk with damaged cholangiocytes (159). HSCs themselves can respond to mechanical pressure by activating and transforming into myofibroblasts during the wound healing process (159).

Recently, the role of mechanically-induced stress and TGF-β1 activation, and subsequent fibrosis, has been clarified through their relationship with the αvβ6 integrin. As mentioned above, integrin-fibronectin complexes can be activated by increased

mechanical stress. Increased binding affinity of $\alpha v\beta 6$ integrin associates with latency-associated peptide, which releases latent TGF-$\beta 1$ and triggers SMAD phosphorylation and nuclear translocation. Wang et al. demonstrated that $\alpha v\beta 6$ integrin expression is highly upregulated in cholangiocytes following acute biliary obstruction, and that lack of $\alpha v\beta 6$ integrin expression ameliorated the fibrotic phenotype. Additionally, $\alpha v\beta 6$ integrin is implicated in potential cholangiocyte EMT, presumably inducing pro-fibrotic fibroblasts (160, 161).

We have shown that loss of $\alpha 7$-nAChR reduces biliary proliferation and fibrosis in response to increased pressure. While there is no previous literature regarding $\alpha 7$-nAChR activity and mechanical stress or integrin physiology specifically in the liver, previous studies have demonstrated that ionic events in nicotinic Ach receptors are linked to keratinocyte locomotion during skin wound healing (162). Thus, the presence of mechanical stress in human and mouse models of liver diseases may be a deciding factor in whether $\alpha 7$-nAChR, and by extension nicotine, is beneficial or malevolent in disease amelioration.

5 CONCLUSIONS[5]

The studies presented here suggest a dichotomous role for the canonical tumor suppressor menin in cholestatic liver disease. On the one hand, menin is positively associated with liver damage and fibrosis in both BDL and MDR2$^{-/-}$ mouse models, specifically via the menin-MLL interaction. However, menin also plays its canonical tumor suppressor role in human CCA, albeit while still driving tumor fibrosis. The findings are problematic because it is believed that cholangiocyte proliferation following injury, termed ductular reaction, is linked to hepatic fibrosis through one or two ways (163). First, proliferating cholangiocytes may undergo an EMT-like change and adopt a pro-fibrotic phenotype, or second, they may secrete signals that activate other cells in the liver, such as fibroblasts, stellate cells, or macrophages, to produce excessive ECM. However, the results reported in this dissertation show that menin can disassociate cholangiocyte proliferation from hepatic fibrosis in cholestatic liver disease.

Following cholestatic liver injury, cholangiocytes become reactive and adopt a neuroendocrine-like phenotype by secreting and responding to a number of peptides in both autocrine and paracrine fashions. Almost all models of biliary injury trigger cholangiocyte proliferation, a process deemed ductular reaction. There are multiple cell types involved in this process, and the type of liver injury determines how ductular reaction takes shape. For example, following bile-duct ligation (BDL) in a mouse model

[5] § Part of this chapter is reprinted with permission from L. Ehrlich, T. Lairmore, G. Alpini, and S. Glaser. Biliary epithelium: Neuroendocrine Compartment in Cholestatic Liver Disease. Clinics and Research in Hepatology and Gastroenterology, 2017. © Elsevier Limited.

for extrahepatic cholestasis, large cholangiocytes respond by undergoing mitosis and proliferating while small cholangiocytes transdifferentiate into large cholangiocytes. Distinct signaling mechanisms regulate these disparate outcomes. In this model, large cholangiocytes respond to increased secretin-secretin receptor cognate interactions to boost intracellular cAMP levels and trigger the PKA/Src/MEK/ERK1/1 pathway (12). In contrast, small cholangiocytes are characterized by activation of the IP3/Ca^{2+}/calmodulin pathway (15).

TGF-β1 plays a major role in fibrosis, proliferation, EMT, and ECM turnover. TGF-β1 lies latent within the extracellular matrix until it is activated by mechanical stress and/or proteolytic cleavage in response to injury or cellular signaling. Once it binds to its cognate receptor (TGF- β1 receptor), it induces phosphorylation of its associated transcription factor, SMAD. Phosphorylated SMADs then translocate to the nucleus where they control gene expression. A direct outcome of TGF-β1 signaling is increased expression, synthesis, and deposition of ECM such as collagen, fibronectin, and proteoglycans. Furthermore, TGF-β1 inhibits matrix metalloproteinases (MMPs) and increases the activity of tissue inhibitors of proteinases (TIMPs) to decrease ECM breakdown (7) (9). An imbalance between MMPs and TIMPs is a major characteristic of fibrosis, with increased TIMP activity greatly increasing ECM deposition.

Previous studies have also painted a conflicting role for menin in HCC and cirrhosis. In one such study, the authors showed that menin interacts with Sirt1 to deacetylate p65 and repress NK-κβ-mediated transcription in order to suppress HCC proliferation (29).

However, another study reported that menin drives HCC formation through menin-MLL-dependent H3K4 trimethylation at key promoter sites, including YAP1 (66). In addition, Zindy et al. established that menin expression increased in human HCC samples from patients with underlying cirrhosis, and increased MEN1 expression activates HSCs in a TGF-β1-dependent manner (32). Given that menin-related hepatic damage and fibrosis is MLL-dependent (marked by histone methylation status), it is probable that menin's tumor suppressive function is related to histone deacetylase activity (which is mediated by the JunD binding partner). Interestingly, JunD and histone deacetylase activity is implicated in oxidative stress, angiogenesis, and RAS-mediated proliferation. JunD activity decreases reactive oxygen species and thus reduces expression of HIF-1alpha and VEGF-A. Menin can bind to the N-terminus of JunD, and loss of menin transforms JunD from a growth suppressor to a growth promoter (164). Thus, it is conceivable that the reduction in angioproliferative markers following miR-24 inhibition/menin overexpression is due to enhanced menin-JunD deacetylase activity.

Furthermore, we have identified the miR-24/menin axis as a suitable target to reduce CCA tumor burden. miR-24 is well documented to negatively regulate menin expression in MEN1 syndrome and drive tumorigenesis (42). There is strong evidence for the oncogenic role of miR-24 in pancreatic ductal adenocarcinoma (PDAC) as well. miR-24 overexpression was shown to decrease FZD5 (WNT receptor), HNF1B (HOX transcription factor), and TMEM92 to drive EMT in PDAC. A separate study showed that miR-24 regulated the BIM pathway to drive PDAC angiogenesis (45, 46). Melatonin

negatively regulates miR-24 expression in several cancers to inhibit tumor proliferation and migration, and lower melatonin signaling in cholangiocytes leads to increased VEGF expression (47). miR-24 expression is increased in HCC and its inhibition reduces proliferation, migration, and invasion (48). Interestingly, miR-24 expression is regulated by menin-MLL dependent histone trimethylation (26).

Another possible explanation for the seemingly dichotomous outcomes of menin expression or function is the cell type through which they function. We have shown, through *in vitro* experiments, that manipulating menin expression in cholangiocytes has a direct effect on proliferation, angiogenesis, migration, and invasion. However, as mentioned above, menin is ubiquitously expressed, and its function is tissue- and pathway-specific. For example, menin interacts with SMADs following TGF-β1 signaling to activate hepatic stellate cells and drive hepatic fibrosis. Menin-HDAC complex can bind and repress the BACH2 locus to prevent senescent and inflammatory CD4+ T cell phenotypes (72). In contrast, menin-MLL drives histone methylation and transcription at Th2 and GATA loci to drive the type II helper T cell phenotype, which is believed to be profibrotic in numerous cholangiopathies (81) (165). Furthermore, menin binds to and drives transcription at IL17 and RORC promoter sites to maintain Th17+ T cell differentiation and function (73). IL17 secretion by Th17+ T cells can trigger hepatic stellate cell activation, collagen deposition, and subsequent hepatic fibrosis (74). Additionally, the menin-MLL interaction drives production of the proinflammatory cytokine CXCl10 in pro-inflammatory M1 macrophages (69). Thus, it is possible that menin drives a fibrotic phenotype through stromal cells but can suppress

epithelial cell tumor proliferation in CCA models.

Another interesting result from these studies is the change in menin expression from early to late stage MDR2$^{-/-}$ mice. As described above, menin expression is decreased (and miR-24 expression increased) in early stage MDR2$^{-/-}$, which then flips in later diseases stages and matches measurements from late stage human PSC samples. However, overexpressing menin through miR-24 Vivo Morpholino treatment increased hepatic fibrosis and biliary proliferation in both early stage MDR2$^{-/-}$ mice and matching FVB/NJ background controls. This indicates that menin downregulation may be a compensatory mechanism in early stage MDR2$^{-/-}$ mice (and possibly early stages of PSC as well). Furthermore, while menin overexpression did increase biliary proliferation, it did not increase expression of proliferative markers in total liver. Similarly, treatment with the menin-MLL inhibitor decreased IBDM but did not change expression of proliferative markers in total liver. This builds the case that menin exerts separate effects on stromal cells (which make up only a small fraction of total liver weight) compared to hepatocytes.

Conversely, menin expression is upregulated in the BDL mouse model, and treatment with a menin-MLL interaction inhibitor abrogates BDL-induced hepatic damage, fibrosis, and biliary proliferation. The difference in menin expression between BDL and MDR2$^{-/-}$ models is perhaps reflective of the different pathophysiologies of the two models. BDL damage is acute and marked by a physical increase of pressure along the biliary tree. Coincidentally our results show that menin expression also increases

following increased mechanical stress in *in vitro* models. (which is abrogated with loss of α7nachr). In the MDR2$^{-/-}$ model, similar to human PSC patients, hepatic fibrosis takes more time to develop. Human PSC patients and MDR2$^{-/-}$ mice share phenotypic and histological properties, but that is where the similarities end. While MDR2$^{-/-}$ is caused by a genetic defect in the ABC4 gene, a canalicular phospholipase that releases phosphatidylcholine into the bile duct lumen in order to form fewer toxic micelles, human PSC has an unknown etiology. There are rare forms of human disease caused by mutation in ABC4, however they manifest as progressive familial intrahepatic cholestasis type 3, low phospholipid associated cholelithiasis, parenteral nutrition-induced cholestasis, sepsis, etc. (165).

Human PSC is considered autoimmune in nature, and certain genetic variations and environmental exposures are believed to increase susceptibility. However, PSC in humans and MDR2$^{-/-}$ mice have different molecular signatures. For example, PSC is characterized by the presence of autoantibodies (p-ANCA) in the serum that is not present in MDR2$^{-/-}$ mice. PSC has a decidedly male prevalence whereas MDR2$^{-/-}$ is gender neutral, and PSC is associated with inflammatory bowel disease, which MDR2$^{-/-}$ is not. Furthermore, PSC increases lifetime risk of developing CCA, whereas MDR2$^{-/-}$ mice develop mixed HCC/CCA tumors. While PSC features dysregulated immune cell populations and altered microbiota, MDR2$^{-/-}$ do not display bacterial translocations relative to FVB/NJ controls. Immune cell populations in MDR2$^{-/-}$ have not been rigorously assessed (166).

In conclusion, we have shown that menin plays an important role in cholestatic liver disease and could potentially be targeted to treat both cholestatic disease (with the menin-MLL inhibitor) and cholangiocarcinoma (with the mIR-24 inhibitor). There remains work to be done. Menin's function is closely tied with a cell's epigenetic state, thus there is a need to characterize epigenetic markers in various disease models. Such studies may help elucidate the tissue- and pathway-specific nature of menin's function. Furthermore, it will be important to delineate how menin affects cholangiocytes as opposed to fibroblasts and immune cells.

REFERENCES

1. Hirschfield GM, Heathcote EJ, Gershwin ME. Pathogenesis of cholestatic liver disease and therapeutic approaches. Gastroenterology 2010;139:1481-1496.

2. Alpini G, Lenzi R, Sarkozi L, Tavoloni N. Biliary physiology in rats with bile ductular cell hyperplasia. Evidence for a secretory function of proliferated bile ductules. J Clin Invest 1988;81:569-578.

3. Alpini G, Roberts S, Kuntz SM, Ueno Y, Gubba S, Podila PV, LeSage G, et al. Morphological, molecular, and functional heterogeneity of cholangiocytes from normal rat liver. Gastroenterology 1996;110:1636-1643.

4. Benedetti A, Bassotti C, Rapino K, Marucci L, Jezequel AM. A morphometric study of the epithelium lining the rat intrahepatic biliary tree. J Hepatol 1996;24:335-342.

5. Glaser S, Gaudio E, Rao A, Pierce L, Onori P, Franchitto A, Francis H, et al. Morphological and Functional Heterogeneity of the Mouse Intrahepatic Biliary Epithelium. Laboratory investigation; a journal of technical methods and pathology 2009;89:456-469.

6. Park SM. The Crucial Role of Cholangiocytes in Cholangiopathies. Gut Liver 2012;6:295-304.

7. Kumar V, Abbas AK, Aster JC. Pathologic Basis of Disease, Ninth Edition Philadelphia, PA Elselvier Saunders, 2015

8. Heathcote EJ. Management of primary biliary cirrhosis. The American Association for the Study of Liver Diseases practice guidelines. Hepatology 2000;31:1005-1013.

9. Lee YA, Wallace MC, Friedman SL. Pathobiology of liver fibrosis: a translational

success story. Gut 2015;64:830-841.

10. Bottcher K, Pinzani M. Pathophysiology of liver fibrosis and the methodological barriers to the development of anti-fibrogenic agents. Adv Drug Deliv Rev 2017.

11. Wells RG. Cellular Sources of Extracellular Matrix in Hepatic Fibrosis. Clinics in liver disease 2008;12:759-viii.

12. Francis H, Glaser S, Ueno Y, Lesage G, Marucci L, Benedetti A, Taffetani S, et al. cAMP stimulates the secretory and proliferative capacity of the rat intrahepatic biliary epithelium through changes in the PKA/Src/MEK/ERK1/2 pathway. J Hepatol 2004;41:528-537.

13. Beuers U, Hohenester S, de Buy Wenniger LJ, Kremer AE, Jansen PL, Elferink RP. The biliary HCO(3)(-) umbrella: a unifying hypothesis on pathogenetic and therapeutic aspects of fibrosing cholangiopathies. Hepatology 2010;52:1489-1496.

14. Glaser S, Meng F, Han Y, Onori P, Chow BK, Francis H, Venter J, et al. Secretin stimulates biliary cell proliferation by regulating expression of microRNA 125b and microRNA let7a in mice. Gastroenterology 2014;146:1795-1808.e1712.

15. Mancinelli R, Franchitto A, Gaudio E, Onori P, Glaser S, Francis H, Venter J, et al. After Damage of Large Bile Ducts by Gamma-Aminobutyric Acid, Small Ducts Replenish the Biliary Tree by Amplification of Calcium-Dependent Signaling and de Novo Acquisition of Large Cholangiocyte Phenotypes. Am J Pathol 2010;176:1790-1800.

16. Karin D, Koyama Y, Brenner D, Kisseleva T. The characteristics of activated portal fibroblasts/myofibroblasts in liver fibrosis. Differentiation 2016;92:84-92.

17. Chandrasekharappa SC, Guru SC, Manickam P, Olufemi S-E, Collins FS, Emmert-

Buck MR, Debelenko LV, et al. Positional Cloning of the Gene for Multiple Endocrine Neoplasia-Type 1. Science 1997;276:404-407.

18. Norton JA, Krampitz G, Jensen RT. Multiple Endocrine Neoplasia: Genetics and Clinical Management. Surg Oncol Clin N Am 2015;24:795-832.

19. Marini F, Giusti F, Brandi ML. Genetic test in multiple endocrine neoplasia type 1 syndrome: An evolving story. World J Exp Med 2015;5:124-129.

20. McCallum RW, Parameswaran V, Burgess JR. Multiple endocrine neoplasia type 1 (MEN 1) is associated with an increased prevalence of diabetes mellitus and impaired fasting glucose. Clin Endocrinol (Oxf) 2006;65:163-168.

21. Lemos MC, Thakker RV. Multiple endocrine neoplasia type 1 (MEN1): analysis of 1336 mutations reported in the first decade following identification of the gene. Hum Mutat 2008;29:22-32.

22. Canaff L, Vanbellinghen JF, Kanazawa I, Kwak H, Garfield N, Vautour L, Hendy GN. Menin missense mutants encoded by the MEN1 gene that are targeted to the proteasome: restoration of expression and activity by CHIP siRNA. J Clin Endocrinol Metab 2012;97:E282-291.

23. Matkar S, Thiel A, Hua X. Menin: a scaffold protein that controls gene expression and cell signaling. Trends Biochem Sci 2013;38:394-402.

24. Agarwal SK, Impey S, McWeeney S, Scacheri PC, Collins FS, Goodman RH, Spiegel AM, et al. Distribution of menin-occupied regions in chromatin specifies a broad role of menin in transcriptional regulation. Neoplasia 2007;9:101-107.

25. Gobl AE, Berg M, Lopez-Egido JR, Oberg K, Skogseid B, Westin G. Menin

represses JunD-activated transcription by a histone deacetylase-dependent mechanism. Biochim Biophys Acta 1999;1447:51-56.

26. Vijayaraghavan J, Maggi EC, Crabtree JS. miR-24 regulates menin in the endocrine pancreas. Am J Physiol Endocrinol Metab 2014;307:E84-92.

27. Wu Y, Feng ZJ, Gao SB, Matkar S, Xu B, Duan HB, Lin X, et al. Interplay between menin and K-Ras in regulating lung adenocarcinoma. J Biol Chem 2012;287:40003-40011.

28. Veniaminova NA, Hayes MM, Varney JM, Merchant JL. Conditional deletion of menin results in antral G cell hyperplasia and hypergastrinemia. Am J Physiol Gastrointest Liver Physiol 2012;303:G752-764.

29. Gang D, Hongwei H, Hedai L, Ming Z, Qian H, Zhijun L. The tumor suppressor protein menin inhibits NF-kappaB-mediated transactivation through recruitment of Sirt1 in hepatocellular carcinoma. Mol Biol Rep 2013;40:2461-2466.

30. Yokoyama A, Somervaille TCP, Smith KS, Rozenblatt-Rosen O, Meyerson M, Cleary ML. The Menin Tumor Suppressor Protein Is an Essential Oncogenic Cofactor for MLL-Associated Leukemogenesis. Cell 2005;123:207-218.

31. Hendy GN, Kaji H, Sowa H, Lebrun JJ, Canaff L. Menin and TGF-beta superfamily member signaling via the Smad pathway in pituitary, parathyroid and osteoblast. Horm Metab Res 2005;37:375-379.

32. Zindy PJ, L'Helgoualc'h A, Bonnier D, Le Bechec A, Bourd-Boitin K, Zhang CX, Musso O, et al. Upregulation of the tumor suppressor gene menin in hepatocellular carcinomas and its significance in fibrogenesis. Hepatology 2006;44:1296-1307.

33. Kaji H, Canaff L, Lebrun JJ, Goltzman D, Hendy GN. Inactivation of menin, a

Smad3-interacting protein, blocks transforming growth factor type beta signaling. Proc Natl Acad Sci U S A 2001;98:3837-3842.

34. Nguyen Q, Anders RA, Alpini G, Bai H. Yes-associated protein in the liver: Regulation of hepatic development, repair, cell fate determination and tumorigenesis. Digestive and Liver Disease 2015;47:826-835.

35. Sowa H, Kaji H, Kitazawa R, Kitazawa S, Tsukamoto T, Yano S, Tsukada T, et al. Menin inactivation leads to loss of transforming growth factor beta inhibition of parathyroid cell proliferation and parathyroid hormone secretion. Cancer Res 2004;64:2222-2228.

36. Kanno N, LeSage G, Glaser S, Alvaro D, Alpini G. Functional heterogeneity of the intrahepatic biliary epithelium. Hepatology 2000;31:555-561.

37. Lazaridis KN, LaRusso NF. The Cholangiopathies. Mayo Clin Proc 2015;90:791-800.

38. Roskams T, Desmet V. Ductular reaction and its diagnostic significance. Semin Diagn Pathol 1998;15:259-269.

39. LaRusso NF, Shneider BL, Black D, Gores GJ, James SP, Doo E, Hoofnagle JH. Primary sclerosing cholangitis: summary of a workshop. Hepatology 2006;44:746-764.

40. Singh S, Talwalkar JA. Primary sclerosing cholangitis: diagnosis, prognosis, and management. Clin Gastroenterol Hepatol 2013;11:898-907.

41. Saadi M, Yu C, Othman MO. A Review of the Challenges Associated with the Diagnosis and Therapy of Primary Sclerosing Cholangitis. J Clin Transl Hepatol 2014;2:45-52.

42. Luzi E, Marini F, Giusti F, Galli G, Cavalli L, Brandi ML. The negative feedback-

loop between the oncomir Mir-24-1 and menin modulates the Men1 tumorigenesis by mimicking the "Knudson's second hit". PLoS One 2012;7:e39767.

43. Fromaget M, Vercherat C, Zhang CX, Zablewska B, Gaudray P, Chayvialle JA, Calender A, et al. Functional characterization of a promoter region in the human MEN1 tumor suppressor gene. J Mol Biol 2003;333:87-102.

44. Liu R, Zhang H, Wang X, Zhou L, Li H, Deng T, Qu Y, et al. The miR-24-Bim pathway promotes tumor growth and angiogenesis in pancreatic carcinoma. Oncotarget 2015;6:43831-43842.

45. Liu Y-X, Long X-D, Xi Z-F, Ma Y, Huang X-Y, Yao J-G, Wang C, et al. MicroRNA-24 Modulates Aflatoxin B1-Related Hepatocellular Carcinoma Prognosis and Tumorigenesis. BioMed Research International 2014;2014:13.

46. Listing H, Mardin WA, Wohlfromm S, Mees ST, Haier J. MiR-23a/-24-induced gene silencing results in mesothelial cell integration of pancreatic cancer. Br J Cancer 2015;112:131-139.

47. Mori F, Ferraiuolo M, Santoro R, Sacconi A, Goeman F, Pallocca M, Pulito C, et al. Multitargeting activity of miR-24 inhibits long-term melatonin anticancer effects. Oncotarget 2016.

48. Ma Y, She XG, Ming YZ, Wan QQ. miR-24 promotes the proliferation and invasion of HCC cells by targeting SOX7. Tumour Biol 2014;35:10731-10736.

49. Ananthanarayanan M, Li Y, Surapureddi S, Balasubramaniyan N, Ahn J, Goldstein JA, Suchy FJ. Histone H3K4 trimethylation by MLL3 as part of ASCOM complex is critical for NR activation of bile acid transporter genes and is downregulated in cholestasis. Am J

Physiol Gastrointest Liver Physiol 2011;300:G771-781.

50. Dhawan S, Dirice E, Kulkarni RN, Bhushan A. Inhibition of TGF-beta Signaling Promotes Human Pancreatic beta-Cell Replication. Diabetes 2016;65:1208-1218.

51. Qian ZY, Peng Q, Zhang ZW, Zhou LA, Miao Y. Roles of Smad3 and Smad7 in rat pancreatic stellate cells activated by transforming growth factor-beta 1. Hepatobiliary Pancreat Dis Int 2010;9:531-536.

52. Ungefroren H, Groth S, Sebens S, Lehnert H, Gieseler F, Fandrich F. Differential roles of Smad2 and Smad3 in the regulation of TGF-beta1-mediated growth inhibition and cell migration in pancreatic ductal adenocarcinoma cells: control by Rac1. Mol Cancer 2011;10:67.

53. Yoo BM, Yeo M, Oh TY, Choi JH, Kim WW, Kim JH, Cho SW, et al. Amelioration of pancreatic fibrosis in mice with defective TGF-beta signaling. Pancreas 2005;30:e71-79.

54. Dooley S, ten Dijke P. TGF-β in progression of liver disease. Cell and Tissue Research 2012;347:245-256.

55. Oertelt S, Lian ZX, Cheng CM, Chuang YH, Padgett KA, He XS, Ridgway WM, et al. Anti-mitochondrial antibodies and primary biliary cirrhosis in TGF-beta receptor II dominant-negative mice. J Immunol 2006;177:1655-1660.

56. Wang YH, Yang W, Yang JB, Jia YJ, Tang W, Gershwin ME, Ridgway WM, et al. Systems biologic analysis of T regulatory cells genetic pathways in murine primary biliary cirrhosis. J Autoimmun 2015;59:26-37.

57. Wu N, Meng F, Invernizzi P, Bernuzzi F, Venter J, Standeford H, Onori P, et al. The secretin/secretin receptor axis modulates liver fibrosis through changes in TGF-beta1 biliary

secretion. Hepatology 2016.

58. Hall C, Sato K, Wu N, Zhou T, Kyritsi T, Meng F, Glaser S, et al. Regulators of Cholangiocyte Proliferation. Gene Expr 2016.

59. Fickert P, Wagner M, Marschall HU, Fuchsbichler A, Zollner G, Tsybrovskyy O, Zatloukal K, et al. 24-norUrsodeoxycholic acid is superior to ursodeoxycholic acid in the treatment of sclerosing cholangitis in Mdr2 (Abcb4) knockout mice. Gastroenterology 2006;130:465-481.

60. Kennedy LL, Meng F, Venter JK, Zhou T, Karstens WA, Hargrove LA, Wu N, et al. Knockout of microRNA-21 reduces biliary hyperplasia and liver fibrosis in cholestatic bile duct ligated mice. Lab Invest 2016;96:1256-1267.

61. Morcos PA, Li Y, Jiang S. Vivo-Morpholinos: a non-peptide transporter delivers Morpholinos into a wide array of mouse tissues. Biotechniques 2008;45:613-614, 616, 618 passim.

62. Onori P, Franchitto A, Alvaro D, Gaudio E. Immunohistochemical features of bile duct epithelial cells in normal and experimental liver conditions. Ital J Anat Embryol 2001;106:371-378.

63. Shattuck TM, Costa J, Bernstein M, Jensen RT, Chung DC, Arnold A. Mutational analysis of Smad3, a candidate tumor suppressor implicated in TGF-beta and menin pathways, in parathyroid adenomas and enteropancreatic endocrine tumors. J Clin Endocrinol Metab 2002;87:3911-3914.

64. Cao Y, Xue Y, Xue L, Jiang X, Wang X, Zhang Z, Yang J, et al. Hepatic menin recruits SIRT1 to control liver steatosis through histone deacetylation. J Hepatol

2013;59:1299-1306.

65. Yang JH, Kim SC, Kim KM, Jang CH, Cho SS, Kim SJ, Ku SK, et al. Isorhamnetin attenuates liver fibrosis by inhibiting TGF-beta/Smad signaling and relieving oxidative stress. Eur J Pharmacol 2016;783:92-102.

66. Xu B, Li SH, Zheng R, Gao SB, Ding LH, Yin ZY, Lin X, et al. Menin promotes hepatocellular carcinogenesis and epigenetically up-regulates Yap1 transcription. Proc Natl Acad Sci U S A 2013;110:17480-17485.

67. Wang J, Huang W, Xu R, Nie Y, Cao X, Meng J, Xu X, et al. MicroRNA-24 regulates cardiac fibrosis after myocardial infarction. J Cell Mol Med 2012;16:2150-2160.

68. Luna C, Li G, Qiu J, Epstein DL, Gonzalez P. MicroRNA-24 regulates the processing of latent TGFbeta1 during cyclic mechanical stress in human trabecular meshwork cells through direct targeting of FURIN. J Cell Physiol 2011;226:1407-1414.

69. Kittan NA, Allen RM, Dhaliwal A, Cavassani KA, Schaller M, Gallagher KA, Carson WFIV, et al. Cytokine Induced Phenotypic and Epigenetic Signatures Are Key to Establishing Specific Macrophage Phenotypes. PLOS ONE 2013;8:e78045.

70. Raggi C, Invernizzi P, Andersen JB. Impact of microenvironment and stem-like plasticity in cholangiocarcinoma: molecular networks and biological concepts. J Hepatol 2015;62:198-207.

71. Fordham JB, Naqvi AR, Nares S. Regulation of miR-24, miR-30b, and miR-142-3p during macrophage and dendritic cell differentiation potentiates innate immunity. J Leukoc Biol 2015;98:195-207.

72. Kuwahara M, Suzuki J, Tofukuji S, Yamada T, Kanoh M, Matsumoto A, Maruyama

S, et al. The Menin-Bach2 axis is critical for regulating CD4 T-cell senescence and cytokine homeostasis. Nat Commun 2014;5:3555.

73. Watanabe Y, Onodera A, Kanai U, Ichikawa T, Obata-Ninomiya K, Wada T, Kiuchi M, et al. Trithorax complex component Menin controls differentiation and maintenance of T helper 17 cells. Proc Natl Acad Sci U S A 2014;111:12829-12834.

74. Tan Z, Qian X, Jiang R, Liu Q, Wang Y, Chen C, Wang X, et al. IL-17A Plays a Critical Role in the Pathogenesis of Liver Fibrosis through Hepatic Stellate Cell Activation. The Journal of Immunology 2013.

75. Katt J, Schwinge D, Schoknecht T, Quaas A, Sobottka I, Burandt E, Becker C, et al. Increased T helper type 17 response to pathogen stimulation in patients with primary sclerosing cholangitis. Hepatology 2013;58:1084-1093.

76. Tanner SM, Staley EM, Lorenz RG. Altered Generation of Induced Regulatory T cells In the FVB.mdr1a(−/−) Mouse Model of Colitis. Mucosal immunology 2013;6:309-323.

77. Roh YS, Park S, Lim CW, Kim B. Depletion of Foxp3+ Regulatory T Cells Promotes Profibrogenic Milieu of Cholestasis-Induced Liver Injury. Dig Dis Sci 2015;60:2009-2018.

78. Schwinge D, von Haxthausen F, Quaas A, Carambia A, Otto B, Glaser F, Höh B, et al. Dysfunction of hepatic regulatory T cells in experimental sclerosing cholangitis is related to IL-12 signaling. Journal of Hepatology.

79. Yang X-P, Jiang K, Hirahara K, Vahedi G, Afzali B, Sciume G, Bonelli M, et al. EZH2 is crucial for both differentiation of regulatory T cells and T effector cell expansion. Scientific Reports 2015;5:10643.

80. Yamada T, Kanoh M, Nabe S, Yasuoka T, Suzuki J, Matsumoto A, Kuwahara M, et al. Menin Plays a Critical Role in the Regulation of the Antigen-Specific CD8+ T Cell Response upon Listeria Infection. J Immunol 2016;197:4079-4089.

81. Yamashita M, Hirahara K, Shinnakasu R, Hosokawa H, Norikane S, Kimura MY, Hasegawa A, et al. Crucial role of MLL for the maintenance of memory T helper type 2 cell responses. Immunity 2006;24:611-622.

82. Nakata Y, Brignier AC, Jin S, Shen Y, Rudnick SI, Sugita M, Gewirtz AM. c-Myb, Menin, GATA-3, and MLL form a dynamic transcription complex that plays a pivotal role in human T helper type 2 cell development. Blood 2010;116:1280-1290.

83. Zen Y, Fujii T, Harada K, Kawano M, Yamada K, Takahira M, Nakanuma Y. Th2 and regulatory immune reactions are increased in immunoglobin G4-related sclerosing pancreatitis and cholangitis. Hepatology 2007;45:1538-1546.

84. Pollheimer MJ, Halilbasic E, Fickert P, Trauner M. Pathogenesis of primary sclerosing cholangitis. Best Practice & Research. Clinical Gastroenterology 2011;25:727-739.

85. Masyuk T, Masyuk A, LaRusso N. MicroRNAs in cholangiociliopathies. Cell Cycle 2009;8:1324-1328.

86. Yamaura Y, Nakajima M, Takagi S, Fukami T, Tsuneyama K, Yokoi T. Plasma microRNA profiles in rat models of hepatocellular injury, cholestasis, and steatosis. PLoS One 2012;7:e30250.

87. Kitano M, Bloomston PM. Hepatic Stellate Cells and microRNAs in Pathogenesis of Liver Fibrosis. J Clin Med 2016;5.

88. He S, Malik B, Borkin D, Miao H, Shukla S, Kempinska K, Purohit T, et al. Menin-MLL inhibitors block oncogenic transformation by MLL-fusion proteins in a fusion partner-independent manner. Leukemia 2016;30:508-513.

89. Razumilava N, Gores GJ. Cholangiocarcinoma. Lancet 2014;383:2168-2179.

90. Komuta M, Govaere O, Vandecaveye V, Akiba J, Van Steenbergen W, Verslype C, Laleman W, et al. Histological diversity in cholangiocellular carcinoma reflects the different cholangiocyte phenotypes. Hepatology 2012;55:1876-1888.

91. Francis H, Alpini G, DeMorrow S. Recent advances in the regulation of cholangiocarcinoma growth. Am J Physiol Gastrointest Liver Physiol 2010;299:G1-9.

92. Alvaro D, Mancino MG, Glaser S, Gaudio E, Marzioni M, Francis H, Alpini G. Proliferating cholangiocytes: a neuroendocrine compartment in the diseased liver. Gastroenterology 2007;132:415-431.

93. Huang J, Gurung B, Wan B, Matkar S, Veniaminova NA, Wan K, Merchant JL, et al. The same pocket in menin binds both MLL and JUND but has opposite effects on transcription. Nature 2012;482:542-546.

94. Agarwal SK, Jothi R. Genome-wide characterization of menin-dependent H3K4me3 reveals a specific role for menin in the regulation of genes implicated in MEN1-like tumors. PLoS One 2012;7:e37952.

95. Kim H, Lee JE, Cho EJ, Liu JO, Youn HD. Menin, a tumor suppressor, represses JunD-mediated transcriptional activity by association with an mSin3A-histone deacetylase complex. Cancer Res 2003;63:6135-6139.

96. Jin S, Mao H, Schnepp RW, Sykes SM, Silva AC, D'Andrea AD, Hua X. Menin

associates with FANCD2, a protein involved in repair of DNA damage. Cancer Res 2003;63:4204-4210.

97. Gallo A, Agnese S, Esposito I, Galgani M, Avvedimento VE. Menin stimulates homology-directed DNA repair. FEBS Lett 2010;584:4531-4536.

98. Walls GV. Multiple endocrine neoplasia (MEN) syndromes. Semin Pediatr Surg 2014;23:96-101.

99. Dreijerink KMA, Mulder KW, Winkler GS, Höppener JWM, Lips CJM, Timmers HTM. Menin Links Estrogen Receptor Activation to Histone H3K4 Trimethylation. Cancer Research 2006;66:4929-4935.

100. Paris PL, Sridharan S, Hittelman AB, Kobayashi Y, Perner S, Huang G, Simko J, et al. An oncogenic role for the multiple endocrine neoplasia type 1 gene in prostate cancer. Prostate Cancer Prostatic Dis 2009;12:184-191.

101. Meng FL, Wang W, Jia WD. Diagnostic and prognostic significance of serum miR-24-3p in HBV-related hepatocellular carcinoma. Med Oncol 2014;31:177.

102. Liu YX, Long XD, Xi ZF, Ma Y, Huang XY, Yao JG, Wang C, et al. MicroRNA-24 modulates aflatoxin B1-related hepatocellular carcinoma prognosis and tumorigenesis. Biomed Res Int 2014;2014:482926.

103. Dong W, Li B, Wang Z, Zhang Z, Wang J. Clinical significance of microRNA-24 expression in esophageal squamous cell carcinoma. Neoplasma 2015;62:250-258.

104. Naito Y, Oue N, Pham TT, Yamamoto M, Fujihara M, Ishida T, Mukai S, et al. Characteristic miR-24 Expression in Gastric Cancers among Atomic Bomb Survivors. Pathobiology 2015;82:68-75.

105. Shimizu Y, Demetris AJ, Gollin SM, Storto PD, Bedford HM, Altarac S, Iwatsuki S, et al. Two new human cholangiocarcinoma cell lines and their cytogenetics and responses to growth factors, hormones, cytokines or immunologic effector cells. Int J Cancer 1992;52:252-260.

106. Miyagiwa M, Ichida T, Tokiwa T, Sato J, Sasaki H. A new human cholangiocellular carcinoma cell line (HuCC-T1) producing carbohydrate antigen 19/9 in serum-free medium. In Vitro Cell Dev Biol 1989;25:503-510.

107. Storto PD, Saidman SL, Demetris AJ, Letessier E, Whiteside TL, Gollin SM. Chromosomal breakpoints in cholangiocarcinoma cell lines. Genes Chromosomes Cancer 1990;2:300-310.

108. Knuth A, Gabbert H, Dippold W, Klein O, Sachsse W, Bitter-Suermann D, Prellwitz W, et al. Biliary adenocarcinoma: Characterisation of three new human tumor cell lines. Journal of Hepatology 1985;1:579-596.

109. Kusaka Y, Tokiwa T, Sato J. Establishment and characterization of a cell line from a human cholangiocellular carcinoma. Res Exp Med (Berl) 1988;188:367-375.

110. Saijyo S, Kudo T, Suzuki M, Katayose Y, Shinoda M, Muto T, Fukuhara K, et al. Establishment of a new extrahepatic bile duct carcinoma cell line, TFK-1. Tohoku J Exp Med 1995;177:61-71.

111. Kanno N, Glaser S, Chowdhury U, Phinizy JL, Baiocchi L, Francis H, LeSage G, et al. Gastrin inhibits cholangiocarcinoma growth through increased apoptosis by activation of Ca2+-dependent protein kinase C-alpha. J Hepatol 2001;34:284-291.

112. Francis H, DeMorrow S, Venter J, Onori P, White M, Gaudio E, Francis T, et al.

Inhibition of histidine decarboxylase ablates the autocrine tumorigenic effects of histamine in human cholangiocarcinoma. Gut 2012;61:753-764.

113. Alpini G, Franchitto A, DeMorrow S, Onori P, Gaudio E, Wise C, Francis H, et al. Activation of Alpha(1)-Adrenergic Receptors Stimulate the Growth of Small Mouse Cholangiocytes via Ca(2+)-dependent Activation of NFAT2 and SP1. Hepatology (Baltimore, Md.) 2011;53:628-639.

114. DeMorrow S, Glaser S, Francis H, Venter J, Vaculin B, Vaculin S, Alpini G. Opposing actions of endocannabinoids on cholangiocarcinoma growth: recruitment of Fas and Fas ligand to lipid rafts. J Biol Chem 2007;282:13098-13113.

115. Han Y, Onori P, Meng F, DeMorrow S, Venter J, Francis H, Franchitto A, et al. Prolonged exposure of cholestatic rats to complete dark inhibits biliary hyperplasia and liver fibrosis. Am J Physiol Gastrointest Liver Physiol 2014;307:G894-904.

116. Francis H, Glaser S, DeMorrow S, Gaudio E, Ueno Y, Venter J, Dostal D, et al. Small mouse cholangiocytes proliferate in response to H1 histamine receptor stimulation by activation of the IP3/CaMK I/CREB pathway. American Journal of Physiology - Cell Physiology 2008;295:C499-C513.

117. Fronza M, Heinzmann B, Hamburger M, Laufer S, Merfort I. Determination of the wound healing effect of Calendula extracts using the scratch assay with 3T3 fibroblasts. J Ethnopharmacol 2009;126:463-467.

118. Alpini G, Invernizzi P, Gaudio E, Venter J, Kopriva S, Bernuzzi F, Onori P, et al. Serotonin Metabolism Is Dysregulated in Cholangiocarcinoma, which Has Implications for Tumor Growth. Cancer Research 2008;68:9184-9193.

119. Yan J, Yang Y, Zhang H, King C, Kan HM, Cai Y, Yuan CX, et al. Menin interacts with IQGAP1 to enhance intercellular adhesion of beta-cells. Oncogene 2009;28:973-982.

120. Yokoyama A. Molecular mechanisms of MLL-associated leukemia. Int J Hematol 2015;101:352-361.

121. Karnik SK, Hughes CM, Gu X, Rozenblatt-Rosen O, McLean GW, Xiong Y, Meyerson M, et al. Menin regulates pancreatic islet growth by promoting histone methylation and expression of genes encoding p27Kip1 and p18INK4c. Proc Natl Acad Sci U S A 2005;102:14659-14664.

122. Gaudio E, Barbaro B, Alvaro D, Glaser S, Francis H, Ueno Y, Meininger CJ, et al. Vascular endothelial growth factor stimulates rat cholangiocyte proliferation via an autocrine mechanism. Gastroenterology 2006;130:1270-1282.

123. Turtoi A, Peixoto P, Castronovo V, Bellahcene A. Histone deacetylases and cancer-associated angiogenesis: current understanding of the biology and clinical perspectives. Crit Rev Oncog 2015;20:119-137.

124. Gerald D, Berra E, Frapart YM, Chan DA, Giaccia AJ, Mansuy D, Pouyssegur J, et al. JunD reduces tumor angiogenesis by protecting cells from oxidative stress. Cell 2004;118:781-794.

125. Yang YJ, Song TY, Park J, Lee J, Lim J, Jang H, Kim YN, et al. Menin mediates epigenetic regulation via histone H3 lysine 9 methylation. Cell Death Dis 2013;4:e583.

126. Lazaridis KN, Strazzabosco M, Larusso NF. The cholangiopathies: disorders of biliary epithelia. Gastroenterology 2004;127:1565-1577.

127. Gouw AS, Clouston AD, Theise ND. Ductular reactions in human liver: diversity at

the interface. Hepatology 2011;54:1853-1863.

128. Slott PA, Liu MH, Tavoloni N. Origin, pattern, and mechanism of bile duct proliferation following biliary obstruction in the rat. Gastroenterology 1990;99:466-477.

129. Glaser SS, Onori P, Wise C, Yang F, Marzioni M, Alvaro D, Franchitto A, et al. Recent advances in the regulation of cholangiocyte proliferation and function during extrahepatic cholestasis. Dig Liver Dis 2010;42:245-252.

130. Fickert P, Pollheimer MJ, Beuers U, Lackner C, Hirschfield G, Housset C, Keitel V, et al. Characterization of animal models for primary sclerosing cholangitis (PSC). J Hepatol 2014;60:1290-1303.

131. The FO, Boeckxstaens GE, Snoek SA, Cash JL, Bennink R, Larosa GJ, van den Wijngaard RM, et al. Activation of the cholinergic anti-inflammatory pathway ameliorates postoperative ileus in mice. Gastroenterology 2007;133:1219-1228.

132. Hiramoto T, Chida Y, Sonoda J, Yoshihara K, Sudo N, Kubo C. The hepatic vagus nerve attenuates Fas-induced apoptosis in the mouse liver via alpha7 nicotinic acetylcholine receptor. Gastroenterology 2008;134:2122-2131.

133. Garcia-Ayllon MS, Silveyra MX, Candela A, Compan A, Claria J, Jover R, Perez-Mateo M, et al. Changes in liver and plasma acetylcholinesterase in rats with cirrhosis induced by bile duct ligation. Hepatology 2006;43:444-453.

134. LeSage G, Alvaro D, Benedetti A, Glaser S, Marucci L, Baiocchi L, Eisel W, et al. Cholinergic system modulates growth, apoptosis, and secretion of cholangiocytes from bile duct-ligated rats. Gastroenterology 1999;117:191-199.

135. Morgan ML, Sigala B, Soeda J, Cordero P, Nguyen V, McKee C, Mouraliderane A,

et al. Acetylcholine induces fibrogenic effects via M2/M3 acetylcholine receptors in non-alcoholic steatohepatitis and in primary human hepatic stellate cells. J Gastroenterol Hepatol 2016;31:475-483.

136. Andersen IM, Tengesdal G, Lie BA, Boberg KM, Karlsen TH, Hov JR. Effects of coffee consumption, smoking, and hormones on risk for primary sclerosing cholangitis. Clin Gastroenterol Hepatol 2014;12:1019-1028.

137. van Erpecum KJ, Smits SJ, van de Meeberg PC, Linn FH, Wolfhagen FH, vanBerge-Henegouwen GP, Algra A. Risk of primary sclerosing cholangitis is associated with nonsmoking behavior. Gastroenterology 1996;110:1503-1506.

138. Hrad V, Abebe Y, Ali SH, Velgersdyk J, Al Hallak M, Imam M. Risk and Surveillance of Cancers in Primary Biliary Tract Disease. Gastroenterol Res Pract 2016;2016:3432640.

139. Tischendorf JJ, Meier PN, Strassburg CP, Klempnauer J, Hecker H, Manns MP, Kruger M. Characterization and clinical course of hepatobiliary carcinoma in patients with primary sclerosing cholangitis. Scand J Gastroenterol 2006;41:1227-1234.

140. Stinton LM, Shaffer EA. Epidemiology of Gallbladder Disease: Cholelithiasis and Cancer. Gut Liver 2012;6:172-187.

141. Jensen K, Afroze S, Ueno Y, Rahal K, Frenzel A, Sterling M, Guerrier M, et al. Chronic nicotine exposure stimulates biliary growth and fibrosis in normal rats. Dig Liver Dis 2013;45:754-761.

142. Martinez AK, Jensen K, Hall C, O'Brien A, Ehrlich L, White T, Meng F, et al. Nicotine Promotes Cholangiocarcinoma Growth in Xenograft Mice. Am J Pathol

2017;187:1093-1105.

143. Getz AM, Visser F, Bell EM, Xu F, Flynn NM, Zaidi W, Syed NI. Two proteolytic fragments of menin coordinate the nuclear transcription and postsynaptic clustering of neurotransmitter receptors during synaptogenesis between Lymnaea neurons. Sci Rep 2016;6:31779.

144. Getz AM, Xu F, Visser F, Persson R, Syed NI. Tumor suppressor menin is required for subunit-specific nAChR alpha5 transcription and nAChR-dependent presynaptic facilitation in cultured mouse hippocampal neurons. Sci Rep 2017;7:1768.

145. Ishii M, Vroman B, LaRusso NF. Isolation and morphologic characterization of bile duct epithelial cells from normal rat liver. Gastroenterology 1989;97:1236-1247.

146. Han Y, Meng F, Venter J, Wu N, Wan Y, Standeford H, Francis H, et al. miR-34a-dependent overexpression of Per1 decreases cholangiocarcinoma growth. J Hepatol 2016;64:1295-1304.

147. Puche JE, Lee YA, Jiao J, Aloman C, Fiel MI, Munoz U, Kraus T, et al. A novel murine model to deplete hepatic stellate cells uncovers their role in amplifying liver damage in mice. Hepatology 2013;57:339-350.

148. Wu N, Meng F, Invernizzi P, Bernuzzi F, Venter J, Standeford H, Onori P, et al. The secretin/secretin receptor axis modulates liver fibrosis through changes in transforming growth factor-beta1 biliary secretion in mice. Hepatology 2016;64:865-879.

149. Ueno Y, Alpini G, Yahagi K, Kanno N, Moritoki Y, Fukushima K, Glaser S, et al. Evaluation of differential gene expression by microarray analysis in small and large cholangiocytes isolated from normal mice. Liver Int 2003;23:449-459.

150. Chiang JYL, Ferrell JM. Bile acid metabolism in liver pathobiology. Gene Expr 2018.

151. Rhoades RA, Bell DR: Autonomic Nervous System In: Medical Physiology: Principles for Clinical Medicine, 4e Baltimore, MD: Wolters Kluwer Business 2013.

152. Soeda J, Morgan M, McKee C, Mouralidarane A, Lin C, Roskams T, Oben JA. Nicotine induces fibrogenic changes in human liver via nicotinic acetylcholine receptors expressed on hepatic stellate cells. Biochem Biophys Res Commun 2012;417:17-22.

153. Kimura K, Tanida M, Nagata N, Inaba Y, Watanabe H, Nagashimada M, Ota T, et al. Central Insulin Action Activates Kupffer Cells by Suppressing Hepatic Vagal Activation via the Nicotinic Alpha 7 Acetylcholine Receptor. Cell Rep 2016;14:2362-2374.

154. Altamirano J, Bataller R. Cigarette smoking and chronic liver diseases. Gut 2010;59:1159-1162.

155. Jensen K, Nizamutdinov D, Guerrier M, Afroze S, Dostal D, Glaser S. General mechanisms of nicotine-induced fibrogenesis. Faseb j 2012;26:4778-4787.

156. Albuquerque EX, Pereira EFR, Alkondon M, Rogers SW. Mammalian Nicotinic Acetylcholine Receptors: From Structure to Function. Physiol Rev 2009;89:73-120.

157. Maroni L, Haibo B, Ray D, Zhou T, Wan Y, Meng F, Marzioni M, et al. Functional and Structural Features of Cholangiocytes in Health and Disease. Cell Mol Gastroenterol Hepatol 2015;1:368-380.

158. Heinrich S, Georgiev P, Weber A, Vergopoulos A, Graf R, Clavien PA. Partial bile duct ligation in mice: a novel model of acute cholestasis. Surgery 2011;149:445-451.

159. Georges PC, Hui JJ, Gombos Z, McCormick ME, Wang AY, Uemura M, Mick R, et

al. Increased stiffness of the rat liver precedes matrix deposition: implications for fibrosis. Am J Physiol Gastrointest Liver Physiol 2007;293:G1147-1154.

160. Wang B, Dolinski BM, Kikuchi N, Leone DR, Peters MG, Weinreb PH, Violette SM, et al. Role of αvβ6 Integrin in Acute Biliary Fibrosis. Hepatology 2007;46:1404-1412.

161. Patsenker E, Popov Y, Stickel F, Jonczyk A, Goodman SL, Schuppan D. Inhibition of Integrin Alphavbeta6 on Cholangiocytes Blocks Tgfbeta Activation and Retards Biliary Fibrosis Progression. Gastroenterology 2008;135:660-670.

162. Chernyavsky AI, Arredondo J, Qian J, Galitovskiy V, Grando SA. Coupling of Ionic Events to Protein Kinase Signaling Cascades upon Activation of α7 Nicotinic Receptor: COOPERATIVE REGULATION OF α(2)-INTEGRIN EXPRESSION AND Rho KINASE ACTIVITY. J Biol Chem 2009;284:22140-22148.

163. Glaser SS, Gaudio E, Miller T, Alvaro D, Alpini G. Cholangiocyte proliferation and liver fibrosis. Expert Rev Mol Med 2009;11:e7.

164. Agarwal SK, Novotny EA, Crabtree JS, Weitzman JB, Yaniv M, Burns AL, Chandrasekharappa SC, et al. Transcription factor JunD, deprived of menin, switches from growth suppressor to growth promoter. Proc Natl Acad Sci U S A 2003;100:10770-10775.

165. Popov Y, Patsenker E, Fickert P, Trauner M, Schuppan D. Mdr2 (Abcb4)-/- mice spontaneously develop severe biliary fibrosis via massive dysregulation of pro- and antifibrogenic genes. J Hepatol 2005;43:1045-1054.

166. Aron JH, Bowlus CL. The immunobiology of primary sclerosing cholangitis. Semin Immunopathol 2009;31:383-397.